

Geological Society of America Bulletin

Detrital-zircon geochronology of the northeastern Tibetan plateau

George E. Gehrels, An Yin and Xiao-Feng Wang

Geological Society of America Bulletin 2003;115, no. 7;881-896
doi: 10.1130/0016-7606(2003)115<0881:DGOTNT>2.0.CO;2

Email alerting services click www.gsapubs.org/cgi/alerts to receive free e-mail alerts when new articles cite this article

Subscribe click www.gsapubs.org/subscriptions/ to subscribe to Geological Society of America Bulletin

Permission request click <http://www.geosociety.org/pubs/copyrt.htm#gsa> to contact GSA

Copyright not claimed on content prepared wholly by U.S. government employees within scope of their employment. Individual scientists are hereby granted permission, without fees or further requests to GSA, to use a single figure, a single table, and/or a brief paragraph of text in subsequent works and to make unlimited copies of items in GSA's journals for noncommercial use in classrooms to further education and science. This file may not be posted to any Web site, but authors may post the abstracts only of their articles on their own or their organization's Web site providing the posting includes a reference to the article's full citation. GSA provides this and other forums for the presentation of diverse opinions and positions by scientists worldwide, regardless of their race, citizenship, gender, religion, or political viewpoint. Opinions presented in this publication do not reflect official positions of the Society.

Notes

Detrital-zircon geochronology of the northeastern Tibetan plateau

George E. Gehrels[†]

Department of Geosciences, University of Arizona, Tucson, Arizona 85721, USA

An Yin[‡]

Department of Earth and Space Sciences, University of California, Los Angeles, California 90095-1567, USA

Xiao-Feng Wang

Chinese Academy of Geological Sciences, Institute of Geomechanics, Beijing, 100081, China

ABSTRACT

U-Pb geochronologic analyses have been conducted on 413 detrital-zircon grains collected from 16 samples in the Altun Shan, Nan Shan, and Qilian Shan. The samples come primarily from quartz arenites and metaturbidites of Middle to Late Proterozoic age and from feldspathic and volcanic clast-rich sandstones of early Paleozoic age. Zircon grains in Proterozoic strata resting on Tarim basement yielded mainly 2.0–1.9 Ga ages, whereas Proterozoic strata of the Qaidam and Qilian terranes yielded mainly ca. 930–820 Ma and ca. 1.9–1.1 Ga ages. The younger grains were apparently shed from local igneous rocks, whereas the grains older than 1.1 Ga were shed from an undetermined continental source. Grains in the lower Paleozoic strata are mainly ca. 500–430 Ma and were shed from nearby plutonic and possibly volcanic rocks that formed in a magmatic arc setting.

Our detrital-zircon ages are consistent with a model (first proposed by E.R. Sobel and N. Arnaud) in which early Paleozoic magmatism occurred within a single northeast-facing magmatic arc that was constructed across an assemblage of Middle to Late Proterozoic accretionary complexes, remnants of magmatic arcs, and shallow-marine strata. This arc system was accreted to the Tarim and Sino-Korean cratons during Silurian–Devonian time. The resulting suture has been reactivated as Tertiary thrust faults that currently define the structural and topographic margin of the Tibetan plateau.

Our data also provide two new estimates

for the offset along the eastern Altyn Tagh fault. A belt of Middle Proterozoic shallow-marine strata is offset by ~400 km, whereas a belt of 490–480 Ma magmatic arc rocks is offset by ~370 km. These values are generally similar to the 350–400 km offset reported in most previous studies.

Keywords: tectonics, continental accretion, continental-margin sedimentation, island arcs, China.

INTRODUCTION

The northeastern part of the Tibetan plateau (Fig. 1) is underlain by a collage of tectonic assemblages that formed in a variety of tectonic environments (Li et al., 1978; Xiong and Coney, 1985; Hsü et al., 1995; Şengör and Natal'in, 1996; Xia et al., 1996; Sobel and Arnaud, 1999; Liu, 1988; Xu et al., 2000; Yin and Harrison, 2000; Yang et al., 2001; Cowgill et al., 2003). These assemblages belong to the Qilian and Qaidam terranes (Fig. 2), which consist predominantly of Middle Proterozoic to early Paleozoic volcanic rocks and volcanic clast-rich strata, mélanges, shallow-marine strata, and widespread granitoids. The Qaidam and Qilian terranes are bounded to the north and east by the Early Proterozoic and Late Archean continental crust of the Tarim and Sino-Korean cratons (Figs. 1 and 2).

Accretion of the Qaidam and Qilian terranes to the Tarim and Sino-Korean cratons is known to have occurred during Silurian–Devonian time (Li et al., 1978; Xiong and Coney, 1985; Hsü et al., 1995; Xia et al., 1996; Şengör and Natal'in, 1996; Sobel and Arnaud, 1999; Xu et al., 2000; Yin and Harrison, 2000; Cowgill et al., 2003). Following this accretionary event, little tectonism is recorded from Devonian through Triassic time. Orogenic activity commenced during middle Mesozoic

deformation, uplift, and erosion (Ritts and Biffi, 2000, 2001; Sobel et al., 2001; Delville et al., 2001), and then, during middle to late Cenozoic time, the region was subjected to dramatic imbrication along thrust faults, uplift and erosion, rapid subsidence of foreland basins, and large-scale strike-slip disruption along the Altyn Tagh fault (Molnar and Tapponnier, 1975; Peltzer and Tapponnier, 1988; Meyer et al., 1996, 1998; Métivier et al., 1998; Tapponnier et al., 1990, 2001).

This study is an attempt to use detrital-zircon geochronologic information from pre-Devonian rocks of the Altun Shan, Nan Shan, and Qilian Shan to help unravel the Paleozoic accretionary history of the region and to place tighter constraints on the amount of offset along the eastern part of the Altyn Tagh fault. Our primary tool involves U-Pb geochronologic analyses of detrital-zircon grains from sandstones (and metasediments) as a means of resolving provenance linkages between various assemblages. Possible linkages are considered with the realizations that most large (>100 µm) detrital zircons are ultimately derived from granitoids (rather than volcanic rocks), that the age of a detrital-zircon grain records crystallization of the source rock and places only a maximum age on deposition of the host strata, and that detrital zircons are highly susceptible to sedimentary recycling given their resistance to mechanical abrasion (Gehrels, 2000). It is also important to realize that this study is reconnaissance in nature, given the size of the study area, the lack of a well-established geologic framework for most of the region, and the relatively small number of analyses (average of 21) performed on most samples. Our objective is accordingly to help establish only first-order aspects of the tectonic development of this complex and poorly known region.

[†]E-mail: ggehrels@geo.arizona.edu.

[‡]E-mail: yin@ess.ucla.edu.

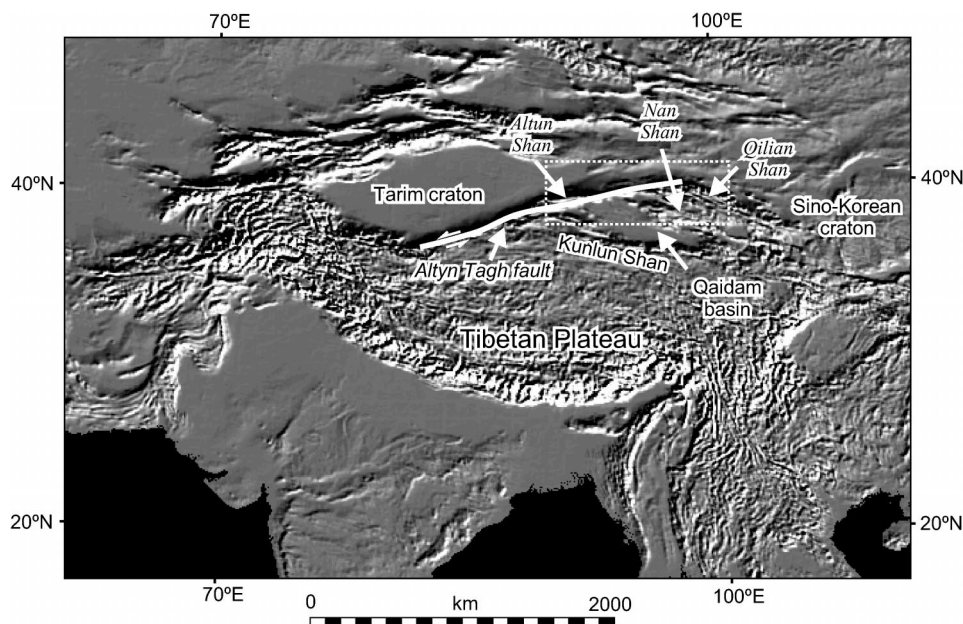


Figure 1. Sketch map showing the location of the study area and the Altyn Tagh fault in the northeastern part of the Tibetan plateau. White rectangle indicates the map area shown in Figure 2. Digital topography from the GLOBE project of the National Geophysical Data Center (<http://www.ngdc.noaa.gov/seg/topo/globe.shtml>).

A companion paper presents the results of U-Pb geochronologic studies of plutons that intrude the terranes (Gehrels et al., 2003). Figure 3 is a summary of the U-Pb ages from Gehrels et al. (2003) and from a similar study by Cowgill et al. (2003) that focuses on the north-central and northwestern parts of the Tibetan plateau.

We have also examined the petrography of the clastic (and metaclastic) samples analyzed for geochronologic information. Although hampered by metamorphism and secondary mineralization, this petrographic information provides a general framework within which the detrital-zircon ages are interpreted.

METHODS

Our geochronologic analyses were conducted on individual detrital-zircon crystals by utilizing conventional isotope-dilution thermal-ionization mass spectrometry (ID-TIMS) for 16 samples, as well as analysis by laser-ablation multicollector inductively coupled plasma-mass spectrometry (LA-MC-ICP-MS) for one sample. These two techniques provide somewhat different information: ID-TIMS analyses yield high-precision ages but are able to identify only the major age components owing to the relatively small numbers of analyses conducted per sample, whereas ICP-MS analyses yield greater errors but allow for a larger number of analyses per sample.

Analytical techniques are described in Appendix 1, and the isotopic data are presented in Tables DR1 and DR2.¹ Note that all ages described in the text have been corrected for common Pb, as denoted by asterisks in $^{206}\text{Pb}^*/^{238}\text{U}$ and $^{207}\text{Pb}^*/^{206}\text{Pb}^*$. Unless otherwise stated, ages younger than 800 Ma are based on $^{206}\text{Pb}^*/^{238}\text{U}$ ratios, whereas ages older than 800 Ma are based on $^{207}\text{Pb}^*/^{206}\text{Pb}^*$ ratios. For ID-TIMS analyses, ages that are >25% discordant (based on comparison of $^{206}\text{Pb}^*/^{238}\text{U}$ and $^{207}\text{Pb}^*/^{206}\text{Pb}^*$ ages) are not included in provenance considerations, with the exception of several grains that clearly belong to a well-defined discordia. For ICP-MS analyses, ages that are >10% discordant or >5% reverse discordant are not included. Analyses that are excluded from further consideration are shown in italic font in Tables DR1 and DR2.

The petrography of the analyzed sandstones and quartzites was determined by point counts ($n > 400$ grains) of each sample, utilizing the Gazzi-Dickinson method (Ingersoll et al., 1984). The framework mineral assemblage is described in Appendix 2 and Table A1, and the results are discussed in the next section and shown in Figure 4.

¹GSA Data Repository item 2003096, Table DR1—Pb/U geochronologic data (TIMS), and Table DR2—Pb/U geochronologic analyses of detrital zircons (LA-MC-ICPMS), is available on the Web at <http://www.geosociety.org/pubs/ft2003.htm>. Requests may also be sent to editing@geosociety.org.

RESULTS OF PETROGRAPHIC STUDIES

Our samples include six sandstones that are quartzose and plot in or near the “continental block” provenance field on QFL and QmFLt diagrams (Fig. 4). These samples were interpreted to be of Proterozoic age (Liu, 1988) because they occur with stromatolite-bearing carbonates and, as described in the next section, yielded primarily Early Proterozoic and Late Archean detrital-zircon ages. These strata are accordingly referred to in the following sections as Proterozoic strata of continental affinity.

Six samples are rich in feldspar grains and in volcanic lithic fragments and lie within the “magmatic arc” provenance field (Fig. 4). These samples are known or inferred to be of early Paleozoic age (Liu, 1988) and yielded detrital zircons that are primarily of early Paleozoic age. They are accordingly referred to as lower Paleozoic strata of magmatic arc affinity.

Four samples contain variable proportions of quartz, feldspar, and volcanic lithic grains and lie within the “recycled orogen” field (Fig. 4). Three of these samples are of early Paleozoic age (Liu, 1988) and yielded detrital-zircon ages ranging from early Paleozoic to Archean. These samples are grouped into a set of lower Paleozoic recycled orogenic sandstones. A fourth sample is of Jurassic age and yielded primarily late Paleozoic detrital-zircon ages. This sample is described in a separate section.

RESULTS OF U-Pb GEOCHRONOLOGIC STUDIES

Detrital zircons have been analyzed from 16 samples. The locations of the samples are described in this section and in Appendix 2 and are shown in Figure 2. Characteristics of the zircons are described in Appendix 2. The age data are shown on concordia diagrams (Figs. 5–6, 8–10, 12–13), plotted on relative-age-probability diagrams (Figs. 7, 11, 14), and presented in detail in Tables DR1 and DR2 (see footnote 1).

Analyses from a rhyolitic sill that provide critical information on the depositional age of the Xorkol sequence are also presented. The age data are shown in Figure 13 and listed in Table DR1 (see footnote 1).

Proterozoic Strata of Continental Affinity

Sample 1

This sample was collected from a thick sequence of reddish quartz arenite beds that are characteristic of the Annanba sequence (Fig. 2). These strata are interlayered with stromat-

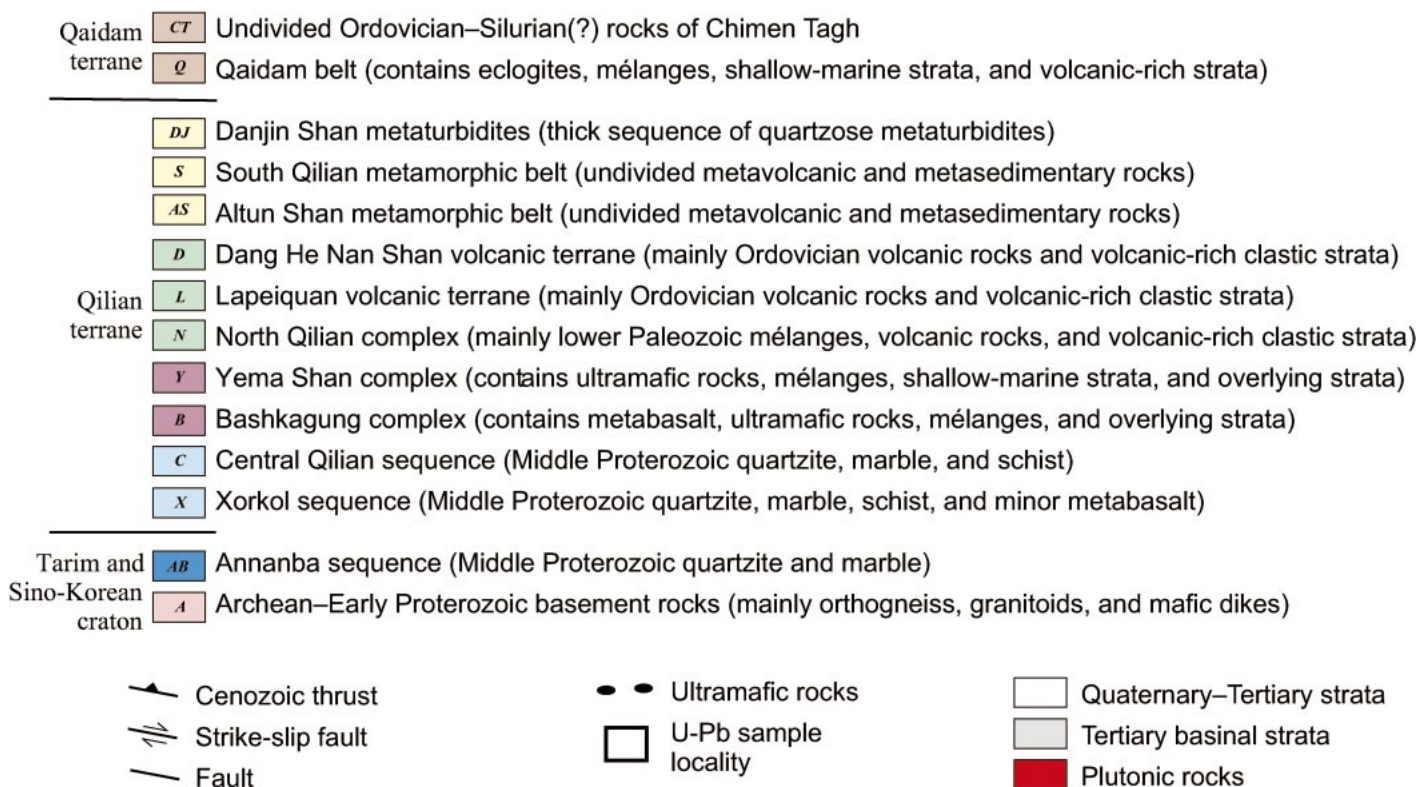
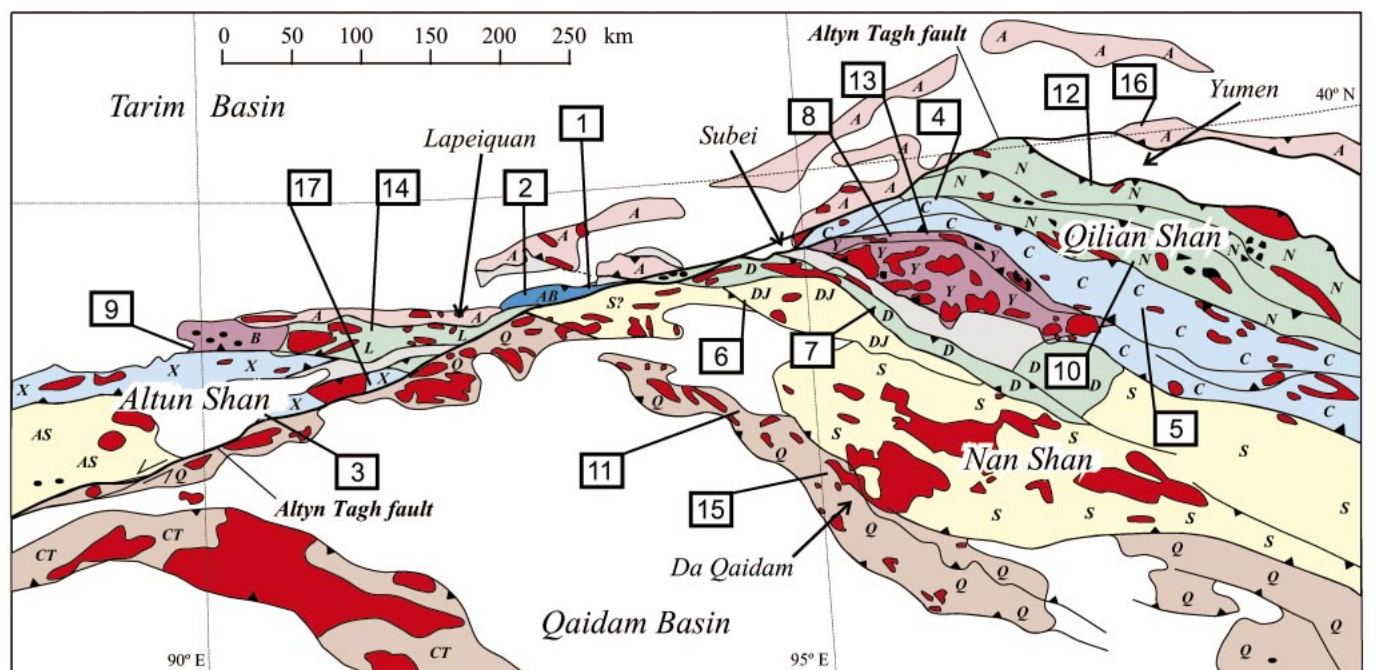


Figure 2. Map of the main tectonic assemblages and first-order structures in the northeastern part of the Tibetan plateau (adapted from Liu [1988]). Geographic names in figure and text are from U.S. Defense Mapping Agency Tactical Pilotage Charts TPC G-8A and G-8B (1:500,000, 1989). Terrane names and divisions are adapted from Yin and Harrison (2000).

olitic marble and rest unconformably on Precambrian basement of the Tarim craton. Liu (1988) assigned a Late Proterozoic age to the sequence, which is consistent with the pres-

ence of stromatolites and the occurrence of zircon grains as young as ca. 1.9 Ga.

Twenty-two abraded zircon grains were analyzed by ID-TIMS. Six concordant grains

and 14 discordant grains yielded a discordia with an upper intercept of 1933 ± 5 Ma and a lower intercept of 687 ± 432 Ma (Fig. 5A). These are interpreted, respectively, as the ages

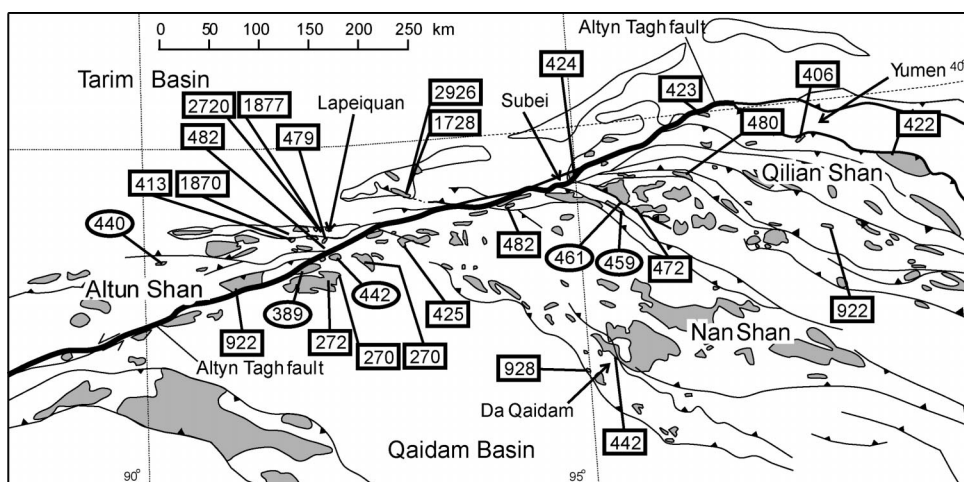


Figure 3. Map showing available U-Pb ages of plutonic rocks in the study area. Base map is simplified from Figure 2. Ages are compiled from Gehrels et al. (2003) and Cowgill et al. (2003).

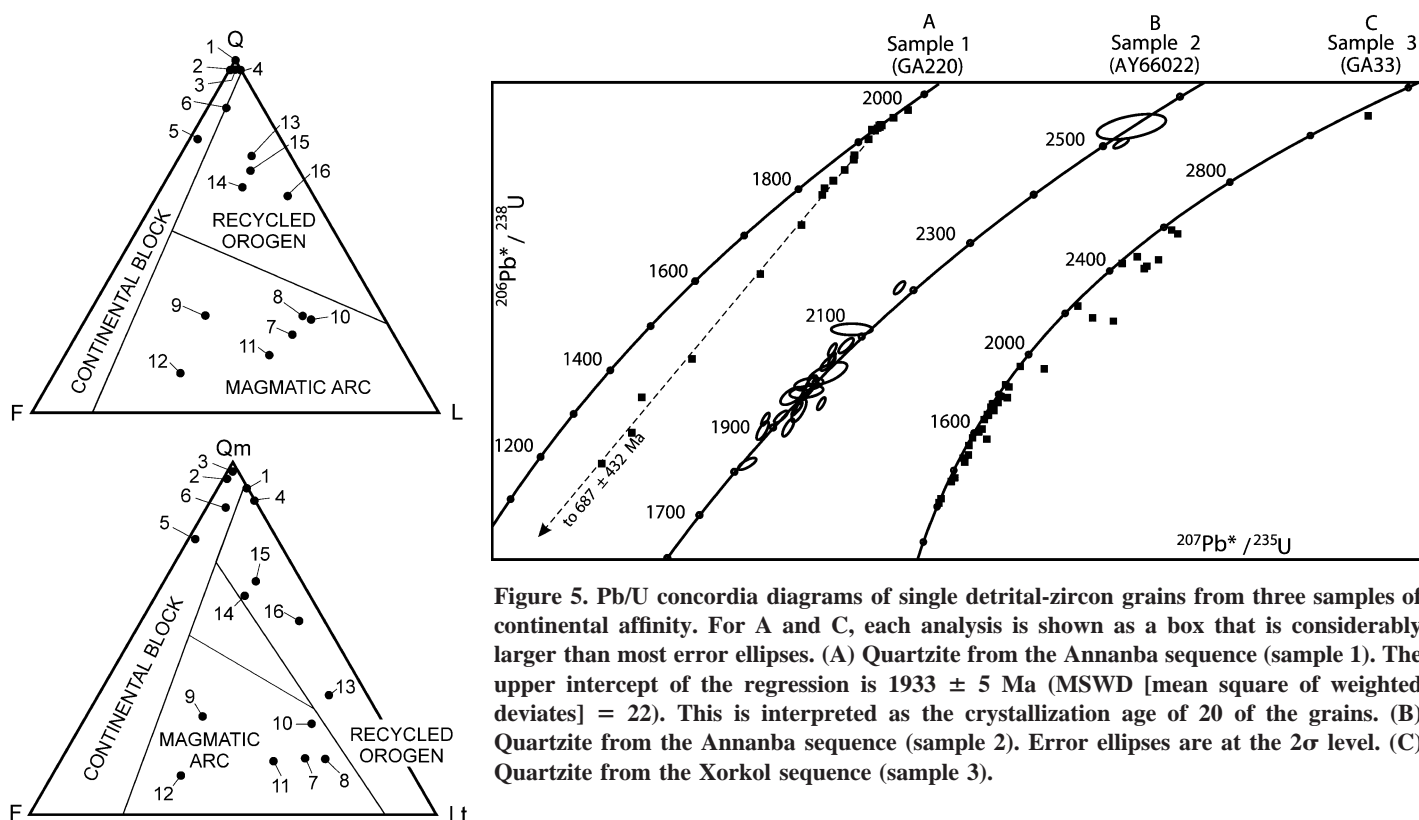


Figure 5. Pb/U concordia diagrams of single detrital-zircon grains from three samples of continental affinity. For A and C, each analysis is shown as a box that is considerably larger than most error ellipses. (A) Quartzite from the Annanba sequence (sample 1). The upper intercept of the regression is 1933 ± 5 Ma (MSWD [mean square of weighted deviates] = 22). This is interpreted as the crystallization age of 20 of the grains. (B) Quartzite from the Annanba sequence (sample 2). Error ellipses are at the 2σ level. (C) Quartzite from the Xorkol sequence (sample 3).

Figure 4. QFL (upper) and QmFLt (lower) diagrams for framework grains in sandstones and quartzites from which detrital zircons have been analyzed. Modes are from Table A1 (Appendix 2); grain types and provenance fields are from Dickinson et al. (1983). Note that framework modes for some samples have large uncertainty owing to grade of metamorphism and/or abundance of secondary minerals (see Appendix 2 for details).

of crystallization and Pb loss. Two additional grains are apparently concordant at ca. 1986 and ca. 1958 Ma. All 22 analyses are included in Figure 7; the ages are 1933 ± 5 Ma ($n = 20$), 1958 ± 7 Ma, and 1986 ± 6 Ma.

Sample 2

This sample was collected from the easternmost Altun Shan, from near the base of the same sedimentary sequence as sample 1 (~20 km to the west). Ninety-five single grains

were analyzed by LA-MC-ICP-MS, of which 60 yielded analyses that are of sufficient precision and concordance that they provide reliable provenance information. These 60 analyses are shown in Figures 5B and 7. The main groups are at ca. 1912 and ca. 1981 Ma (Fig. 7).

Sample 3

This sample was collected from an ~20-m-thick layer of quartzite exposed in the Altun

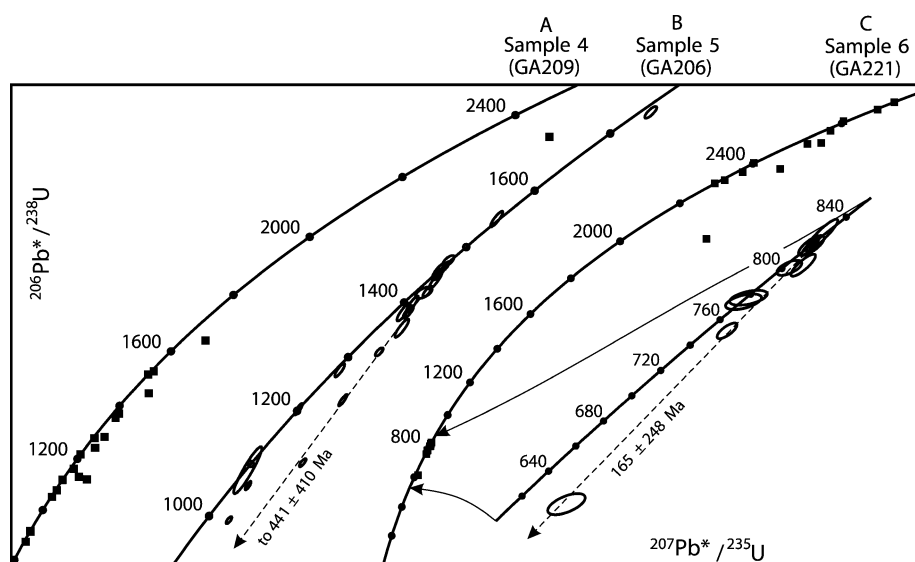


Figure 6. Pb/U concordia diagrams of single detrital-zircon grains from three samples of continental affinity. Note that error ellipses are at the 2σ level. (A) Quartzite from the Central Qilian sequence (sample 4). (B) Quartzite from the Central Qilian sequence (sample 5). The upper intercept of the regression is 1469 ± 12 Ma (MSWD = 6.8). (C) Schistose quartzite from the Danjin Shan metaturbidite unit (sample 6). The upper intercept of the regression is 823 ± 16 Ma (MSWD = 3.7).

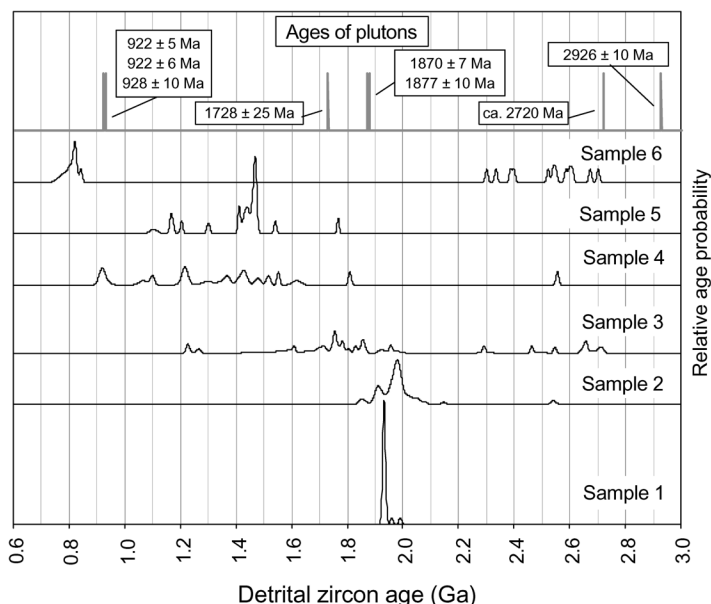


Figure 7. Relative-age-probability diagram comparing ages of detrital-zircon grains from six samples of continental affinity (black curves). Also shown in gray bars are Pb/U ages of Precambrian plutonic rocks from the region, dated by Gehrels et al. (2003). Note that the relative-age-probability curves show ages and uncertainties (plotted as a normal distribution about the age) from each sample. Curves are normalized such that they all contain the same area. The numbers of grains included are 22 (sample 1), 60 (sample 2), 43 (sample 3), 20 (sample 4), 22 (sample 5), and 21 (sample 6).

Shan (Fig. 2). These rocks are interbedded with stromatolitic marble, pelitic schist, and minor mafic metavolcanic rocks of the Xorkol sequence, which were assigned to the Middle Proterozoic Jixian System by Liu (1988). This age assignment is supported by the presence of a 930 ± 10 Ma rhyolitic sill (sample 18) and a 922 ± 6 Ma granitic pluton (sample 6 of Gehrels et al., 2003) (Fig. 3) that intrude the sequence.

Forty-three abraded zircon grains were analyzed by ID-TIMS; their ages range from concordant to highly discordant (Fig. 5C). The main age clusters occur at ca. 1.3–1.2 Ga and ca. 2.0–1.7 Ga (the peak is at ca. 1756 Ma), and there are scattered ages from ca. 2.7 to ca. 2.3 Ga. Figure 7 includes all 43 analyses, plotted according to their $^{207}\text{Pb}^*/^{206}\text{Pb}^*$ ages (Table DR1; see footnote 1).

Sample 4

This sample was collected from an ~200-m-thick clastic sequence consisting of reddish, fine-grained sandstone and greenish mudstone and shale. These rocks are bounded above and below by thick sequences of gray, stromatolitic limestone. Our sample was collected from a medium-grained sandstone layer exposed in the northwestern Qilian Shan (Fig. 2). These strata are part of the Central Qilian sequence (Fig. 2); they were assigned to the Middle Proterozoic Changcheng System by Liu (1988).

Twenty zircon grains were analyzed by ID-TIMS; their ages are concordant to slightly discordant. Three grains are concordant at ca. 930 Ma, and the rest are scattered between ca. 1.6 and ca. 1.0 Ga (Fig. 6A). Figure 7 is a plot of the $^{207}\text{Pb}^*/^{206}\text{Pb}^*$ ages (Table DR1; see footnote 1) of all 20 analyses.

Sample 5

This sample was collected from a 200-m-thick sequence of tan sandstone beds that are overlain and underlain by greenish mudstone and siltstone. The clastic strata are capped by a thick layer of gray stromatolitic limestone, and the base of the sequence is intruded by a granite body that yielded an age of 922 ± 5 Ma (sample 7 of Gehrels et al., 2003) (Fig. 3). Our sample consists of medium-grained sandstone collected from the central Qilian Shan (Fig. 2). These rocks are included in the Central Qilian sequence (Fig. 2) and were assigned a Middle Proterozoic age by Liu (1988).

Twenty-two abraded grains were analyzed by ID-TIMS; their ages range from ca. 1.1 to ca. 1.8 Ga. Several grains lie along a discordia with intercepts of 1469 ± 12 Ma and $441 \pm$

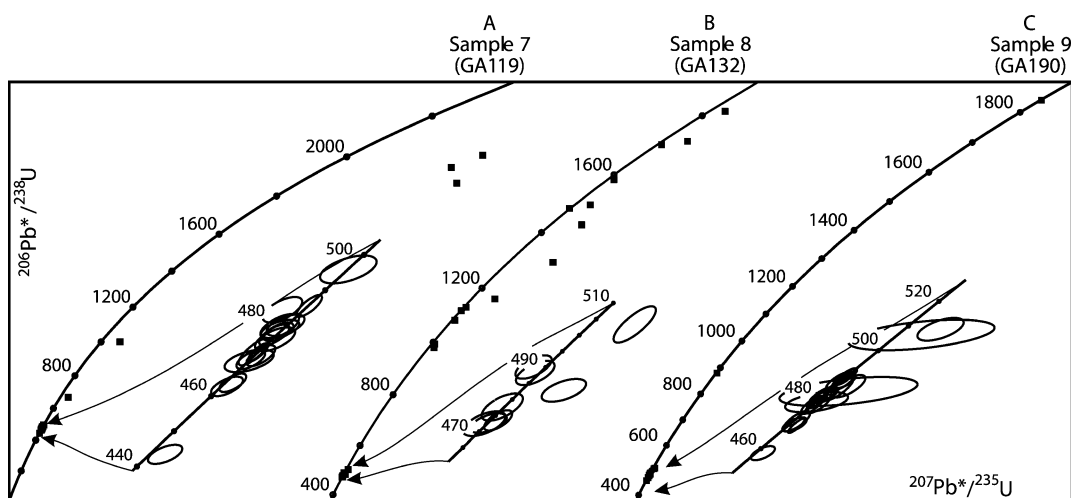


Figure 8. Pb/U concordia diagrams of single detrital-zircon grains from three samples of magmatic arc affinity. Note that error ellipses are at the 2σ level. (A) Sample of sandstone from the Dang He Nan Shan volcanic terrane (sample 7). The youngest grain is interpreted to be discordant owing to Pb loss and is excluded from further consideration. (B) Sample of sandstone from the Yema Shan complex (sample 8). (C) Sample of sandstone from the Bashkagang complex (sample 9).

410 Ma (Fig. 6B). The upper intercept is interpreted as an approximate age of crystallization for these grains. Figure 7 shows the $^{207}\text{Pb}^*/^{206}\text{Pb}^*$ ages (Table DR1; see footnote 1) of all 22 grains.

Sample 6

This sample was collected from a thick sequence of metaturbidites that occurs in the northwestern Nan Shan (Fig. 2). These rocks are shown as the Danjin Shan metaturbidites in Figure 2; they were assigned an early Paleozoic age by Liu (1988).

Twenty-one grains were abraded prior to analysis by ID-TIMS. Most grains yielded concordant to slightly discordant ages that cluster into two general groups. One set defines a discordia with an upper intercept (interpreted as the crystallization age) of 823 ± 16 Ma and a lower intercept of 165 ± 248 Ma (Fig. 6C). Older grains range from ca. 2.7 to ca. 2.3 Ga. Figure 7 shows the $^{207}\text{Pb}^*/^{206}\text{Pb}^*$ ages (Table DR1; see footnote 1) of all 21 grains.

Lower Paleozoic Strata of Magmatic Arc Affinity

Sample 7

This sample was collected from a grayish-green volcanic clast-rich feldspathic wacke exposed in the northwestern Nan Shan (Fig. 2). This sandstone makes up much of the Dang He Nan Shan volcanic terrane (Fig. 2) and was assigned a Late Ordovician age by Liu (1988).

Twenty-two abraded grains were analyzed

by ID-TIMS, 17 of which cluster between 496 and 443 Ma (Fig. 8A). Two grains yielded $^{207}\text{Pb}^*/^{206}\text{Pb}^*$ ages of ca. 2.6–2.5 Ga, and three grains are sufficiently discordant that they are not considered further (Table DR1; see footnote 1). Figure 11 accordingly shows 19 of the 22 ages.

Sample 8

This sample was collected from the northwestern Qilian Shan in a sequence mapped as lower Proterozoic by Liu (1988). We have included these strata in the Yema Shan complex (Fig. 2), which consists of Proterozoic(?) mélangé overlain by lower Paleozoic volcanic clast-rich strata. The younger strata consist mainly of grayish-green volcanic clast-rich feldspathic wacke that contains distinctive bluish quartz grains.

Eight large ($\sim 175 \mu\text{m}$) grains and 14 small ($\sim 80 \mu\text{m}$) grains were analyzed by ID-TIMS. Only the larger grains were abraded. The ages of these grains are correlated with their size: larger grains yielded $^{206}\text{Pb}^*/^{238}\text{U}$ ages of 504–472 Ma, whereas smaller grains yielded $^{207}\text{Pb}^*/^{206}\text{Pb}^*$ ages of ca. 1.2–1.0 and ca. 1.9–1.4 Ga (Fig. 8B). All 22 grains are included in the relative-age-probability plot (Fig. 11).

Sample 9

This sample was collected from a thick sequence of Lower Ordovician (Liu, 1988) sandstone beds in the northern Altun Shan (Fig. 2). These strata are included in the Bashkagang complex, which consists of variably disrupted Proterozoic rocks overlain unconformably by lower Paleozoic volcanic rocks and

volcanic clast-rich clastic strata (Fig. 2). Our sample was collected from near the base of the sequence, where it overlies mafic volcanic rocks and mélangé.

Twenty-two abraded grains were analyzed by ID-TIMS, nearly all of which are concordant (Fig. 8C). Most grains cluster between ca. 500 and ca. 460 Ma (peak age probability at 482 Ma), and there are two older grains at ca. 1840 Ma and ca. 900 Ma. All 22 grains are included in the relative-age-probability plot (Fig. 11).

Sample 10

This sample was collected from Lower Ordovician (Liu, 1988) conglomeratic graywacke that is exposed in the central Qilian Shan (Fig. 2). These strata are included in the North Qilian complex of the Qilian terrane (Fig. 2).

Eleven grains were analyzed by ID-TIMS. Analyses yielded concordant to slightly discordant ages that lie along a discordia with intercepts at 484 ± 5 Ma and 20 ± 184 Ma (Fig. 9A). The upper intercept is interpreted as the probable age of crystallization. All 11 grains are plotted at 484 ± 5 Ma in Figure 11.

Sample 11

This sample was collected from moderately metamorphosed, volcanic clast-rich feldspathic wacke that is interlayered with marble, metabasalt, and metapelite. These rocks are included in the Qaidam belt of the Qaidam terrane (Fig. 2). Liu (1988) assigned the sequence a Late Ordovician age.

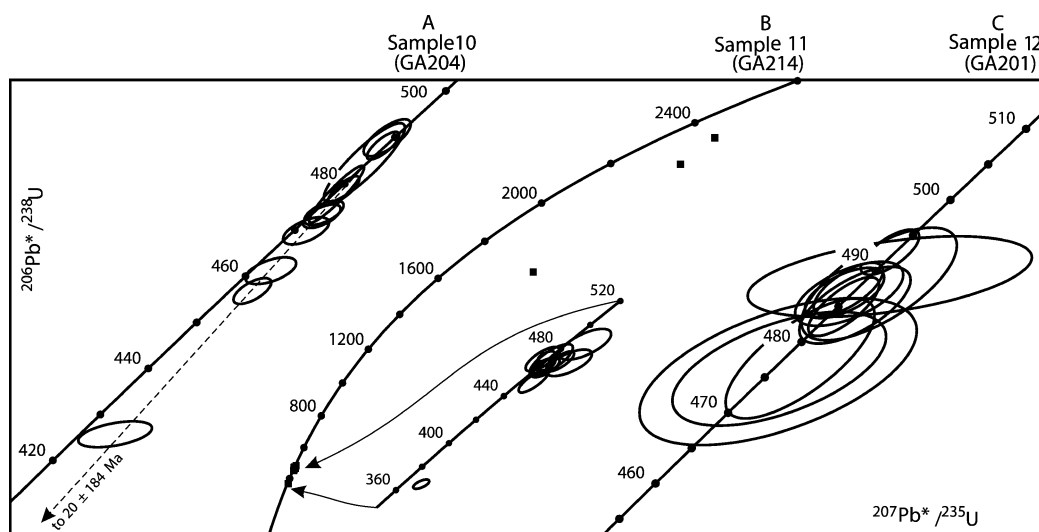


Figure 9. Pb/U concordia diagrams of single detrital-zircon grains from three samples of magmatic arc affinity. (A) Sandstone from the North Qilian complex (sample 10). The upper intercept of the regression, interpreted as the likely crystallization age of most grains, is 484 ± 5 Ma (MSWD = 0.2). (B) Sample of sandstone from the Qaidam belt (sample 11). (C) Sample of sandstone from the North Qilian complex (sample 12).

Thirteen grains were analyzed by ID-TIMS; the ages are between 488 Ma and 453 Ma (age peak at ca. 469 Ma), two older grains of ca. 2.6–2.5 Ga, and two grains that are interpreted to be discordant owing to Pb loss (Fig. 9B). Figure 11 plots all analyses except for the two discordant grains.

Sample 12

This sample was collected from a sequence of volcanic clast-rich, feldspathic turbidites exposed along the eastern flank of the northern Qilian Shan near Yumen (Fig. 2). These strata continue southward into rocks shown as Silurian by Liu (1988) and are included in the North Qilian complex in Figure 2. Eleven abraded grains were analyzed by ID-TIMS, yielding ages between 493 Ma and 476 Ma and an age peak at ca. 486 Ma (Figs. 9C and 11).

Lower Paleozoic Recycled Orogenic Sandstones

Sample 13

This sample was collected from a volcanic clast-rich feldspathic wacke exposed in the northwestern Qilian Shan (Fig. 2). Liu (1988) interpreted these rocks as having an Early Proterozoic age, whereas our mapping suggests that the strata are lower Paleozoic and rest unconformably on a mélange of cherty argillite containing lenses of jadeite-bearing amphibolite, glaucophane schist, and marble. Rocks of the underlying mélange are intruded along strike by a nondeformed granite body that yielded a

U-Pb age of 480 ± 6 Ma (Gehrels et al., 2003) (Fig. 3). Both assemblages are included in the Yema Shan complex in Figure 2.

Twenty-one grains were analyzed by ID-TIMS, all of which were abraded prior to analysis. The ages define two groups that correlate with the characteristics of the grains: 10 colorless, euhedral grains yielded ages that range between 495 Ma and 435 Ma (age peak at ca. 474 Ma), a slightly older grain is discordant owing to inheritance, and 11 pinkish, rounded grains yielded ages that range from ca. 1.6 to ca. 1.0 Ga (Figs. 10A). Figure 11 plots the ages for 20 grains, excluding the discordant analysis with obvious inheritance.

Sample 14

This sample consists of fine-grained, volcanic clast-rich, quartzofeldspathic wacke collected from the Lapeiquan volcanic terrane in the eastern Altun Shan (Fig. 2). Liu (1988) interpreted these strata as Middle Proterozoic in age (Jixian System), whereas our ages demonstrate that the strata are considerably younger.

Twenty-two grains were analyzed by ID-TIMS; all were abraded prior to analysis. Most ages are discordant and lie along a discordia with intercepts of 917 ± 25 Ma and 399 ± 97 Ma (Fig. 10B). There is also one grain at ca. 487 Ma and two grains between ca. 1.2 and ca. 1.0 Ga. Figure 11 shows 19 grains at 917 ± 25 Ma as well as the three other analyses.

Sample 15

This sample was collected from a 10-m-thick conglomeratic horizon that rests (unconformably?) on a sequence of metarhyolite and metabasalt in the western Nan Shan (Fig. 2). These lower Paleozoic (Liu, 1988) strata belong to the Qaidam belt (Fig. 2).

Twenty-seven grains were analyzed by ID-TIMS; all were abraded. The ages yielded two groups at 442–413 Ma (age peak at 434 Ma) and 811–648 Ma ($^{207}\text{Pb}^*/^{206}\text{Pb}^*$ ages) and a scatter of ages from ca. 2.7 to ca. 1.1 Ga (Figs. 10C and 11). Figure 11 shows the ages of all 27 analyses.

Jurassic Strata of the Sino-Korean Craton

Sample 16

This sample was collected from conglomeratic sandstone beds that are exposed in low hills north of Yumen (Fig. 2). These strata were mapped by Liu (1988) as occurring near the base of a Jurassic sequence that rests unconformably on Precambrian crystalline rocks. Because of this map relationship, we interpreted these strata to have been derived primarily from the Precambrian basement rocks. The sample was collected in an effort to obtain a detrital-zircon reference for these basement rocks, which belong to the Sino-Korean craton (Fig. 1).

Nineteen grains were analyzed by ID-TIMS, and all were abraded prior to analysis. Most analyses are concordant; the ages range from 286 Ma to 254 Ma (15 grains) and from 475 Ma to 435 Ma (four grains) (Fig. 12). The

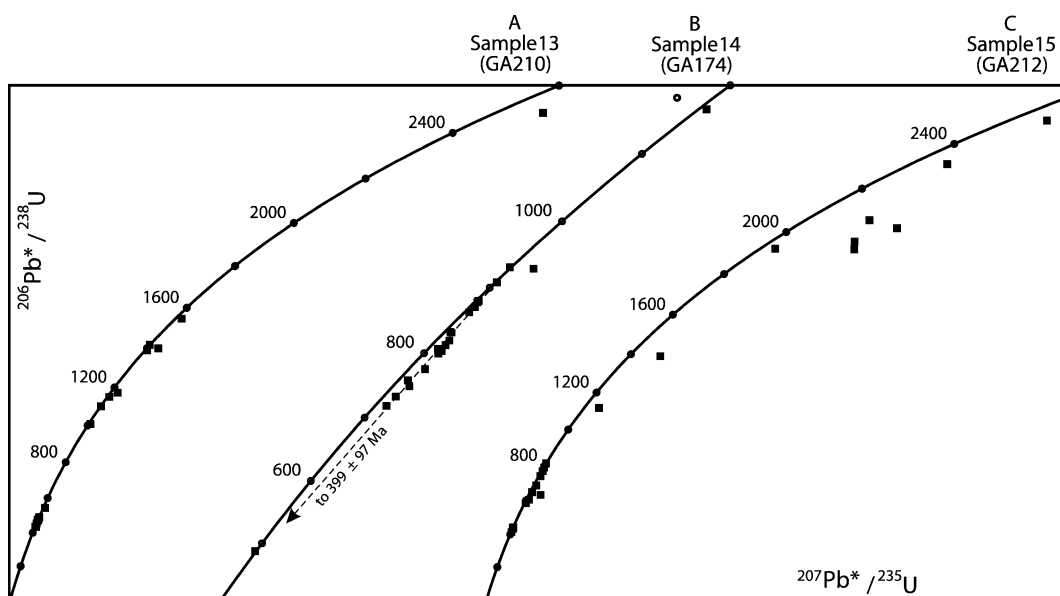


Figure 10. Pb/U concordia diagrams of single detrital-zircon grains from three samples of recycled orogenic provenance. (A) Sample of sandstone from the Yema Shan complex (sample 13). (B) Sample of sandstone from the Lapeiquan volcanic terrane (sample 14). The regression has an upper intercept, interpreted as the likely age of most grains, of 917 ± 25 Ma (MSWD = 17). (C) Sample of quartzite from the Qaidam belt (sample 15).

lack of Precambrian ages in this sample suggests that the contact with crystalline rocks may be a fault rather than an unconformity.

Metarhyolite Sill in the Xorkol Sequence

Sample 17

This sample was collected from a metarhyolite sill that intrudes the Xorkol sequence, which is exposed in the Altun Shan (Fig. 2). Liu (1988) assigned these strata to the Middle Proterozoic Jixian System.

Four colorless grains and two fractions of four light pink grains were analyzed by ID-TIMS. All six analyses are concordant at 930 ± 10 Ma (Fig. 13).

PROVENANCE OF THE DETRITAL ZIRCONS

Proterozoic Strata of Continental Affinity

Geologic relationships (Liu, 1988), combined with the detrital-zircon data presented herein and the U-Pb ages of plutonic rocks in the region (summarized in Fig. 3), indicate that three different Proterozoic stratigraphic assemblages exist in the study area.

Northeasternmost is a sequence of quartzite and stromatolite-bearing marble, referred to as the Annanba sequence (Fig. 2), which rests unconformably on Precambrian basement of the Tarim craton. The detrital-zircon ages from

quartzite layers within the sequence (samples 1 and 2) are generally consistent with this interpretation, given the abundance of Early Proterozoic ages in the quartzites and in Tarim basement rocks (Fig. 7).

A second assemblage is represented by the Central Qilian and Xorkol sequences (Fig. 2). These sequences are dominated by marble, quartzite, and pelitic schist, which presumably accumulated in a shallow-marine environment. Most strata are interpreted to be Middle Proterozoic in age given the occurrence of (1) stromatolites in interlayered marbles in both sequences, (2) quartzites in the Xorkol sequence that have detrital zircons as young as ca. 1220 Ma (Fig. 7) but that are intruded by 930–920 Ma igneous rocks (sample 18 and the 922 Ma age in the Altun Shan in Fig. 3), and (3) strata in the Central Qilian sequence that yielded detrital zircons as young as ca. 1100 Ma (Fig. 7) and that are intruded by a ca. 922 Ma granite body (shown in central Qilian Shan in Fig. 3).

The pre-1.1 Ga detrital zircons in these strata were presumably shed from a continental region dominated by 1.6–1.4 Ga crystalline rocks and containing subordinate 1.9–1.1 Ga rocks (Fig. 7). The Tarim and Sino-Korean cratons are not likely sources for these detrital zircons, because, as shown in Figure 7, such ages are not common in the crystalline basement or in the overlying Annanba sequence. Likely possibilities, based on continental

constructions for Late Proterozoic time by Scotese (2002), include Australia, North China, South China, or nearby continental fragments (Fig. 15).

The similarity of detrital-zircon ages from the Central Qilian and Xorkol sequences, combined with similarities in their stratigraphy and magmatic history, suggests that these two assemblages were continuous prior to offset along the Altyn Tagh fault (Fig. 2). The implications of this correlation for offset on the Altyn Tagh fault are explored in a subsequent section in this paper.

The third assemblage is the Danjin Shan metaturbidites, which is a thick sequence of metasedimentary rocks that underlies a large region of the northwestern Nan Shan and probably continues to the southeast (included within the South Qilian metamorphic belt) (Fig. 2). The source of zircons in this sequence is also uncertain, as there are no obvious local sources for the dominant ca. 820 Ma and ca. 2.7–2.3 Ga detrital-zircon grains (Fig. 7). As with the Xorkol and Central Qilian sequences, a paleoposition in the vicinity of Australia, North China, and South China (Fig. 15) is possible.

Lower Paleozoic Strata of Magmatic Arc and Recycled Orogenic Provenance

Most of our samples come from lower Paleozoic assemblages that include or are dom-

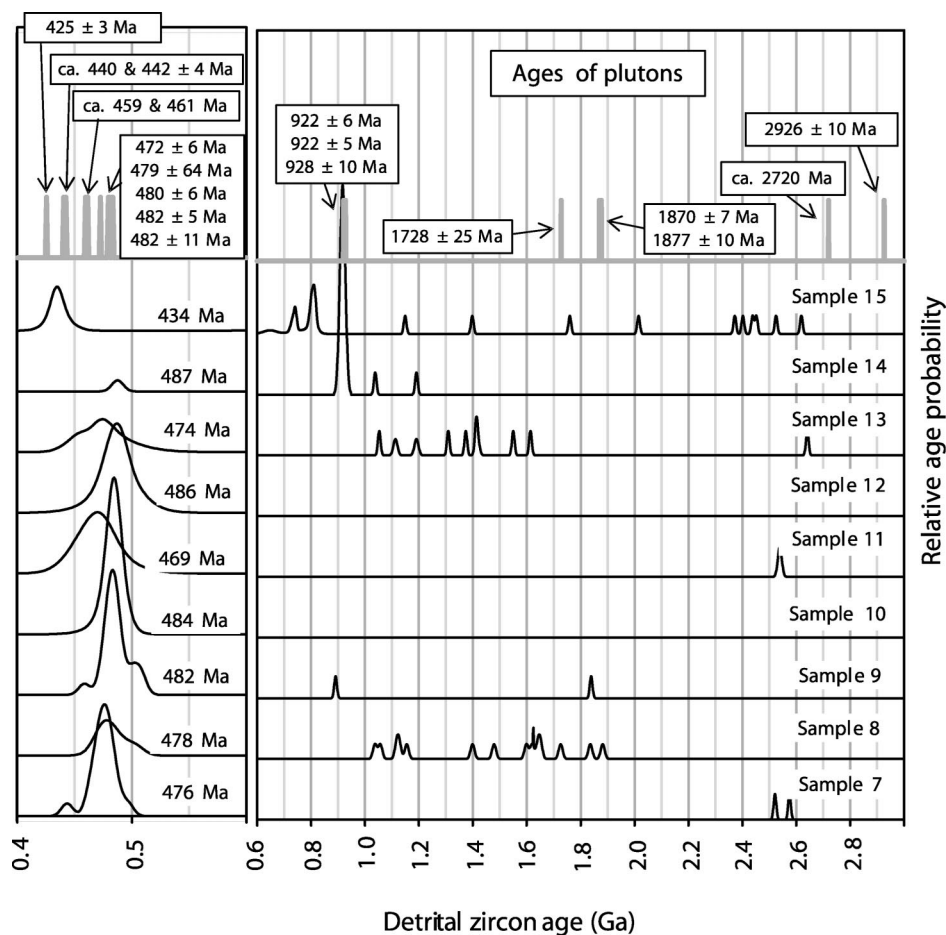


Figure 11. Relative-age-probability diagram comparing ages of detrital-zircon grains from samples of magmatic arc affinity and recycled orogenic provenance (black curves). Peak age probabilities are shown for the younger grains. Also shown in gray bars are Pb/U ages of plutonic rocks from the region, dated by Gehrels et al. (2003) and Cowgill et al. (2003). The numbers of grains included are 22 (sample 7), 22 (sample 8), 22 (sample 9), 11 (sample 10), 12 (sample 11), 11 (sample 12), 20 (sample 13), 22 (sample 14), and 27 (sample 15).

inated by volcanic rocks and volcanic clast-rich sedimentary rocks. Petrographically, these sandstones (and their metamorphic equivalents) are rich in detrital feldspar grains and/or volcanic lithic fragments and lie in the magmatic arc and recycled orogenic provenance fields on QFL and QmFLt diagrams (Fig. 4). Although the sampled assemblages and sandstones are rich in volcanic material, most of the zircons analyzed were probably derived from subvolcanic intrusions that were uplifted and eroded during or soon after the volcanism.

Previous workers concluded that these strata accumulated primarily in oceanic arc settings during early Paleozoic time (Li et al., 1978; Xiong and Coney, 1985; Hsü et al., 1995; Xia et al., 1996; Şengör and Natal'in, 1996; Sobel and Arnaud, 1999; Xu et al., 2000; Yin and

Harrison, 2000). This interpretation is supported by our geochronologic analyses, which show that most strata contain predominantly early Paleozoic detrital zircons (Fig. 11). Of the 10 samples analyzed, eight (samples 7–14) yielded age peaks from 492 to 469 Ma and thus record a predominance of magmatism during Early Ordovician time (according to the time scale of Tucker and McKerrrow, 1995). This result corresponds well with the ages of granitoids that intrude the sampled sequences, which range from 482 to 459 Ma (Figs. 3 and 11).

These samples also contain older detrital zircons whose ages are mostly in the ca. 1.9 Ga to ca. 800 Ma and ca. 2.7 to ca. 2.3 Ga ranges. The occurrence of ca. 900 Ma grains in samples 9 and 14 (from the Lapeiquan and Bashkagung sequences in the Altun Shan)

suggests a provenance link with igneous rocks in the nearby Xorkol sequence (Fig. 11). The occurrence of abundant ca. 1.9–1.0 Ga detrital-zircon grains in samples 8 and 13 (both from the Yema Shan complex) suggests either derivation from continental rocks of these ages or, more likely, recycling of grains from quartzites of the nearby Central Qilian sequence.

One of the samples, from the Qaidam belt in the western Nan Shan (sample 15), records slightly younger magmatism with an age peak at 434 Ma (Late Ordovician–early Silurian time). This age corresponds well with the ca. 442 and ca. 425 Ma ages of plutonic rocks nearby (Figs. 3 and 11). This sample also contains older zircons with age clusters at ca. 810 Ma and ca. 2.7–2.3 Ga (Fig. 10C). These ages have not been recognized in igneous rocks in the region, but match well with the ages of detrital zircons in the nearby Danjin Shan metaturbidites (Figs. 6C and 7). Hence, it is likely that Ordovician–Silurian strata in the western Nan Shan were derived from contemporaneous magmatic sources and from nearby Middle to Late Proterozoic metasedimentary basement.

The relationship between the early Paleozoic detrital-zircon ages and the ages of plutonism in the region is explored in Figure 16. The study area is divided into three regions that contain detrital-zircon “peak” ages and pluton ages between 490 and 478 Ma, between 478 and 450 Ma, and between 450 and 425 Ma. Of the 20 ages appropriate for comparison, only two do not fit these within these broad age bands. The apparent decrease in age southwestward, particularly south of the Altyn Tagh fault, is interpreted as a record of magmatism migrating from northeast to southwest through Ordovician–early Silurian time. North of the fault, the band of 490–478 Ma magmatism can be traced with confidence, but the younger bands are not as obvious (Fig. 16).

Jurassic Strata

The ca. 285–255 Ma and ca. 475 Ma detrital zircons in Jurassic strata near Yumen (sample 16, Fig. 2) were most likely shed from plutons of these ages in the northeastern part of the Tibetan plateau. Igneous rocks of ca. 475 Ma are widespread in the region, whereas ca. 285–255 Ma granite bodies are known in the study area only from the northern margin of the Qaidam basin (Fig. 3; Gehrels et al., 2003). Late Paleozoic granitoids are also widespread in the Kunlun Shan (Harris et al., 1988). This coarse clastic detritus apparently accumulated during a widespread uplift and

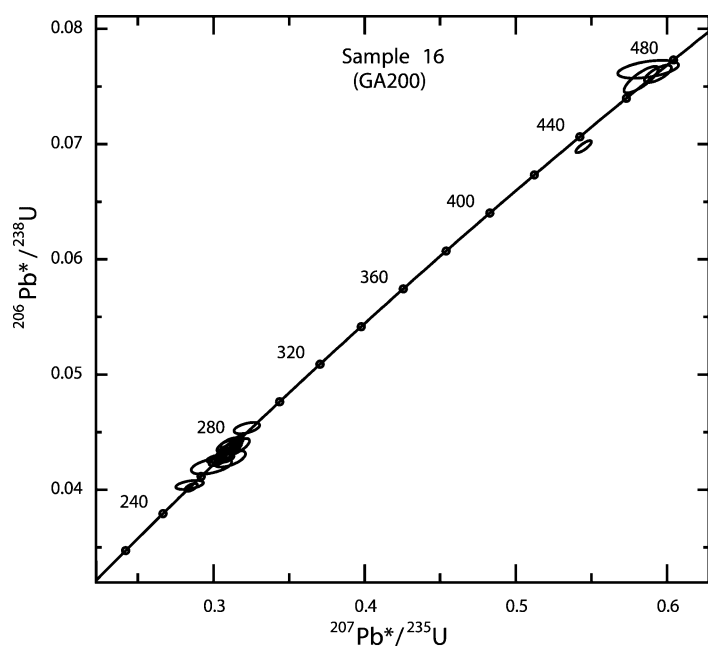


Figure 12. Pb/U concordia diagram of single detrital-zircon grains from a sample of sandstone from Jurassic strata north of Yumen (sample 16).

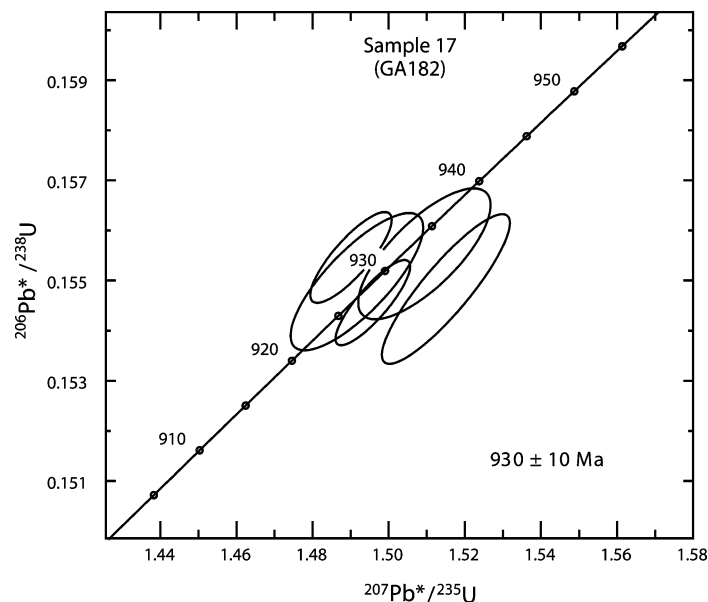


Figure 13. Pb/U concordia diagram of zircon grains from a sample of a metarhyolite sill from the Xorkol sequence (sample 17).

erosional event of Jurassic age (Ritts and Biffi, 2000, 2001; Sobel et al., 2001; Delville et al., 2001).

IMPLICATIONS FOR PALEOZOIC ACCRETIONARY HISTORY

Accretion of the Qaidam and Qilian terranes to the Tarim and Sino-Korean cratons

is known to have occurred during Silurian–Devonian time, as Devonian and younger platform strata unconformably overlie all terranes and the adjacent craton (Li et al., 1978; Xiong and Coney, 1985; Liu, 1988; Hsü et al., 1995; Xia et al., 1996; Şenğör and Natal'in, 1996; Xu et al., 2000; Yin and Harrison, 2000; Cowgill et al., 2003). There is considerable debate, however, about the pre-Devonian con-

figuration of the terranes and their boundaries and about the tectonic processes by which the terranes were accreted. Three main models are discussed here.

Archipelago Model

According to Li et al. (1978), Xiong and Coney (1985), Hsü et al. (1995), Xia et al. (1996), Xu et al. (2000), and Yin and Harrison (2000), the Qilian and Qaidam terranes consist of four separate volcanic arc complexes that were separated from each other and from the Tarim and Sino-Korean cratons by separate ocean basins during early Paleozoic time (Fig. 17A). Xu et al. (2000), Yin and Harrison (2000), and Yang et al. (2001) suggested that these basins closed along northeast-dipping (using present coordinates) subduction zones, forming early Paleozoic volcanic arc systems on each of the terranes and along the southern margin of the craton to the north. In contrast, Li et al. (1978), Xiong and Coney (1985), and Hsü et al. (1995) interpreted the convergent margins to have faced both northeast and southwest, whereas Xia et al. (1996) suggested that the arcs faced northeastward.

Our data are inconsistent with a multiple-arc model for two reasons:

1. Provenance links appear to exist between most of the assemblages in the Qaidam and Qilian terranes, as follows: 1.9–1.1 Ga detrital-zircon grains are common in strata of the Xorkol, Central Qilian, and Yema Shan assemblages; 930–920 Ma detrital grains occur in the Bashkagung, Lapeiquan, and Central Qilian assemblages, whereas granitoids of the same age occur in the Xorkol, Central Qilian, and Qaidam assemblages (Fig. 3); and ca. 820 Ma detrital-zircon grains are common in strata from both the Qaidam and Danjin Shan assemblages (Figs. 7 and 11). These data suggest that the Qaidam terrane and much of the Qilian terrane together make up a single crustal fragment, rather than several separate arc terranes.

2. As shown in Figure 16, magmatism appears to have swept southwestward across the Qilian and Qaidam terranes during Ordovician and Early Silurian time. This is not a pattern that would be expected in a series of unrelated magmatic arcs.

Broad Accretionary Complex

Şenğör and Natal'in (1996) suggested that the Qaidam and Qilian terranes consist of a single broad convergent-margin assemblage that formed along the margin of the Tarim and Sino-Korean cratons. The assemblage grew

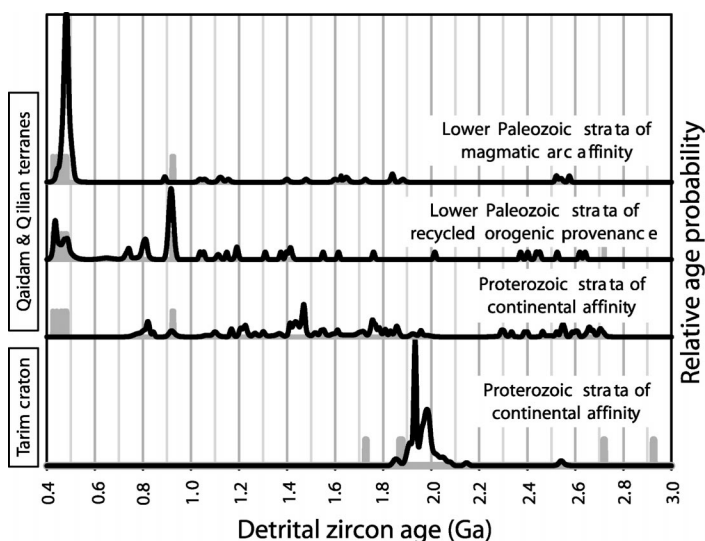


Figure 14. Relative-age-probability diagram comparing ages of detrital-zircon grains and plutons from the main tectonic assemblages analyzed in this study. The lower curve shows age information for detrital-zircon grains from the Annanba sequence (samples 1–2, black curve) and for plutonic rocks in the Tarim craton (gray bars). The upper three curves show age information for detrital-zircon grains (black curves) from additional strata of continental affinity (samples 3–6), from Paleozoic strata of recycled orogenic provenance (samples 13–15), and from Paleozoic strata of magmatic arc affinity (samples 7–12). Pb/U ages of granitoids in the Qilian and Qaidam terranes are shown in the upper three curves with gray bars (ages from Gehrels et al. [2003] and Cowgill et al. [2003]).

southwestward during early Paleozoic time by the progressive addition of accretionary complexes and magmatic arcs in a southwest-facing convergent margin (Fig. 17B).

Our data are consistent with this model in that magmatism migrated southwestward during Ordovician–early Silurian time (Fig. 16). The following aspects of our geochronologic data, however, are inconsistent with this model:

1. Strata in the Qaidam and Qilian terranes yielded detrital zircons that were clearly shed from a continental source region, but the disparity in ages suggests a source other than the Tarim and Sino-Korean cratons.

2. The regional occurrence of Mesoproterozoic quartz arenites containing continent-derived detrital zircons (Xorkol and Central Qilian sequences) is not consistent with formation along an early Paleozoic accretionary margin.

3. Our detrital-zircon data suggest that magmatism occurred in the region at 930–920 Ma and ca. 820 Ma. The 930–920 Ma ages coincide with the emplacement of granitoids of the same age in the Xorkol, Central Qilian, and Qaidam assemblages. This timing suggests that arc-type(?) magmatism was widespread in the region long before the early Pa-

leozoic convergence described by Şengör and Natal'in (1996).

4. As described by Gehrels et al. (2003), the ca. 920 Ma granite body in the Qaidam terrane intrudes eclogites that are interpreted to have formed in an accretionary complex (Yang et al., 2001). These relationships demonstrate that, at least in this area, formation of an accretionary complex significantly predated early Paleozoic time.

Northeast-Facing Magmatic Arc

Sobel and Arnaud (1999) suggested that a single arc system formed in response to southwest-dipping subduction beneath the northeastern margin of the Qilian terrane in the Altun Shan. Closure of this northeast-facing subduction system is interpreted to have produced a single throughgoing suture along the leading edge of this segment of the Qilian terrane.

Three different aspects of our data support the model of Sobel and Arnaud (1999) and suggest that this suture continues eastward through the North Qilian complex of the northeastern Qilian Shan (Fig. 2):

1. In strata of the Qaidam and Qilian terranes, the scarcity of detritus older than 1.9

Ga suggests that the strata accumulated in proximity to a continental mass other than the Tarim and Sino-Korean cratons. The location of the Tertiary thrust faults that mark (a) the present northern and eastern boundaries of the North Qilian, Lapeiquan, and Bashkagung assemblages (Fig. 2), and (b) the topographic and structural margin of the northeastern Tibetan plateau may therefore coincide with an early Paleozoic suture along the inboard margin of the Qaidam and Qilian terranes.

2. The regional occurrence of 1.9–1.1 Ga, 930–920 Ma, and ca. 820 Ma detrital-zircon grains in the Qaidam and Qilian terranes (Figs. 7 and 11) suggests that the entire region was a single coherent crustal fragment during early Paleozoic time.

3. The pattern of Ordovician–early Silurian magmatism sweeping southwestward across the Qaidam and Qilian terranes (Fig. 16) is supportive of the region having formed a single crustal fragment during early Paleozoic time.

On the basis of these lines of evidence, we propose the Late Proterozoic–early Paleozoic tectonic history shown in Figures 17C–17E. During Early Ordovician time, subduction occurred along the northeastern margin (using present coordinates) of a large crustal fragment comprising the Qilian and Qaidam terranes (Fig. 17C). Subduction may have also occurred along the southwestern margin of this fragment, forming a separate Kunlun arc. During Middle Ordovician through Early Silurian time the magmatism migrated southwestward, producing the younger plutons and arc-derived sandstones in the Qaidam–South Qilian belts (Fig. 17D). Accretion began during middle Silurian time and continued into the Early Devonian, as recorded by the presence of ca. 424–406 Ma accretion-related plutons in the North Qilian terrane (Gehrels et al., 2003) and ca. 435–383 Ma cooling ages of plutons in the Altun Shan (Sobel and Arnaud, 1999) (Fig. 17E). Additional studies of the age of accretionary complexes within and between the Qaidam and Qilian terranes would provide critical tests of this model.

IMPLICATIONS FOR OFFSET ON THE ALTYN TAGH FAULT

Many different offset markers have been used to provide estimates of the total left-lateral offset on the Altyn Tagh fault. For the central and western segments of the fault, Peltzer and Tapponnier (1988) reported that Paleozoic plutons in the western Kunlun Shan have been offset by ~500 km from their equivalents on the north side of the fault.

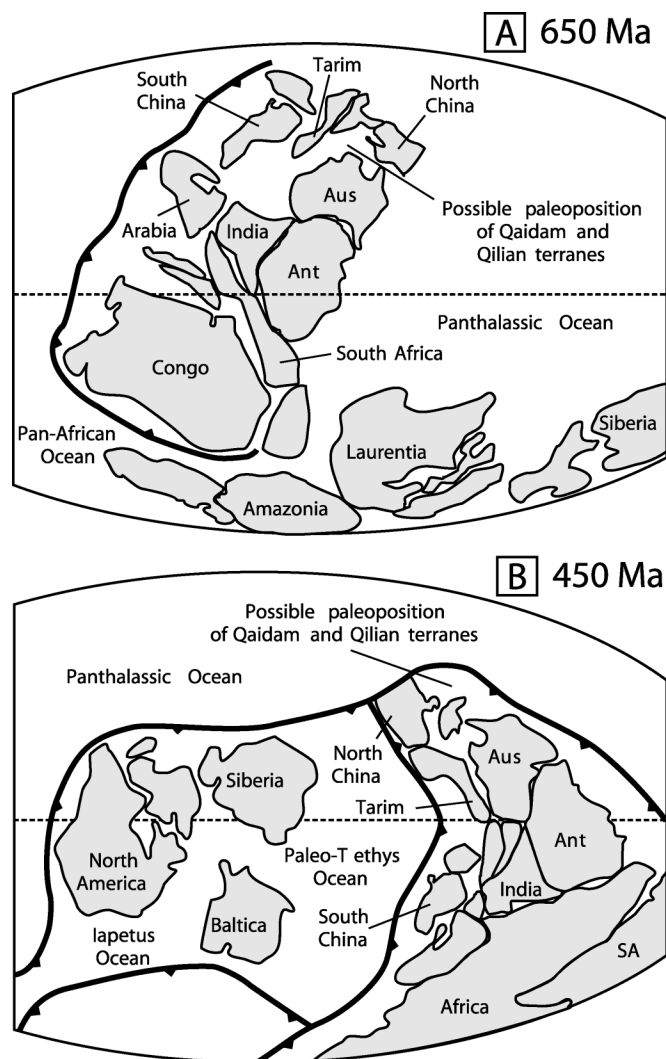


Figure 15. Continental reconstructions showing possible positions for rocks in the Altun Shan, Nan Shan, and Qilian Shan during (A) Late Proterozoic time and (B) early Paleozoic time. Maps are adapted from reconstructions of Scotese (2002).

Cowgill et al. (2003) have reevaluated this offset marker with improved age constraints and have concluded that the displacement is 475 ± 70 km. Offset estimates on the eastern segment of the fault include (1) ~ 400 km, on the basis of a general comparison of the geology of the Altyn Tagh with the Nan Shan and Qilian Shan (Molnar and Tapponnier, 1975); 400 ± 60 km, on the basis of the offset of Jurassic shoreline deposits (Ritts and Biffi, 2000); (3) 280 ± 30 km, on the basis of correlation of Tertiary thrust faults and Tertiary basin strata across the fault (Yin and Harrison, 2000); (4) ~ 350 km, on the basis of patterns of Jurassic cooling ages (Sobel et al., 2001); (5) 375 ± 25 km, on the basis of connecting Tertiary conglomeratic strata southwest of Lapeiquan (Fig. 2) with probable source terranes in the northwestern Qilian Shan (Yue et

al., 2001); and (6) ~ 400 km, on the basis of matching metamorphic assemblages across the fault (Yang et al., 2001).

Two aspects of our data provide new information on the amount of offset along the eastern segment of the fault. The first constraint is a correlation between the Xorkol and Central Qilian sequences, which is based on similarities in both stratigraphic characteristics and detrital-zircon ages. Projection of centerlines through the outcrop bands of the Xorkol and Central Qilian sequences in Figure 2 to the Altyn Tagh fault yields an offset of ~ 400 km. This determination has significant but poorly constrained uncertainty, given that the outcrop bands of the two sequences are based on the geometry of Tertiary thrust faults, rather than reflecting pre-Tertiary structural or stratigraphic features. A second offset marker

is provided by the patterns of early Paleozoic magmatism on either side of the fault. As shown in Figure 16, projection of the position of ca. 490–478 Ma magmatism yields an offset of ~ 370 km. This offset marker also has significant uncertainty due to projection of these early Paleozoic features along the structural grain defined by Tertiary thrust faults and due to the scarcity of age information north of the fault.

CONCLUSIONS

Although reconnaissance in nature, our detrital-zircon analyses yielded several first-order conclusions regarding the tectonic history of the northeastern Tibetan plateau. The first-order conclusions are as follows:

1. Rocks in the Altun Shan, Qilian Shan, and Nan Shan record widespread arc-type magmatism during Ordovician and Early Silurian time. This tectonic setting is reflected in the composition of the lower Paleozoic sandstones analyzed, which are generally of magmatic arc or recycled orogenic provenance on QFL and QmFLt diagrams (Fig. 4). These sandstones yielded detrital-zircon ages that range from ca. 490–480 Ma in the northeastern part of the study area to ca. 440–430 to the southwest (Fig. 16). These ages match well with the U-Pb ages of plutons in the region, which also young to the southwest (Gehrels et al., 2003; Cowgill et al., 2003). These age trends apparently record southwestward (in present coordinates) migration of arc-related magmatism. This magmatism apparently shut off at ca. 425 Ma, just prior to accretion of the Qaidam and Qilian terranes onto the margin of the Tarim and Sino-Korean cratons (Sobel and Arnaud, 1999; Gehrels et al., 2003).

2. The lower Paleozoic strata accumulated on and adjacent to a heterogeneous basement complex that includes a thick sequence of Neoproterozoic(?) metaturbidites, Mesoproterozoic (930–920 Ma) granitoids, shallow-marine quartzite and marble that accumulated between ca. 1100 and ca. 920 Ma, and ultramafic rocks, high-pressure assemblages (including eclogitic rocks), and mélangé that are at least locally intruded by the 930–920 Ma granitoids. Samples of the metaturbidites and the shallow-marine quartzites are all of continental affinity on QFL and QmFLt diagrams (Fig. 4) and yielded detrital zircons that range from ca. 1.9 to ca. 1.1 Ga (mainly ca. 1.6–1.4 Ga) (Fig. 11). These ages are not consistent with derivation from the adjacent Tarim and Sino-Korean cratons; likely alternatives in-

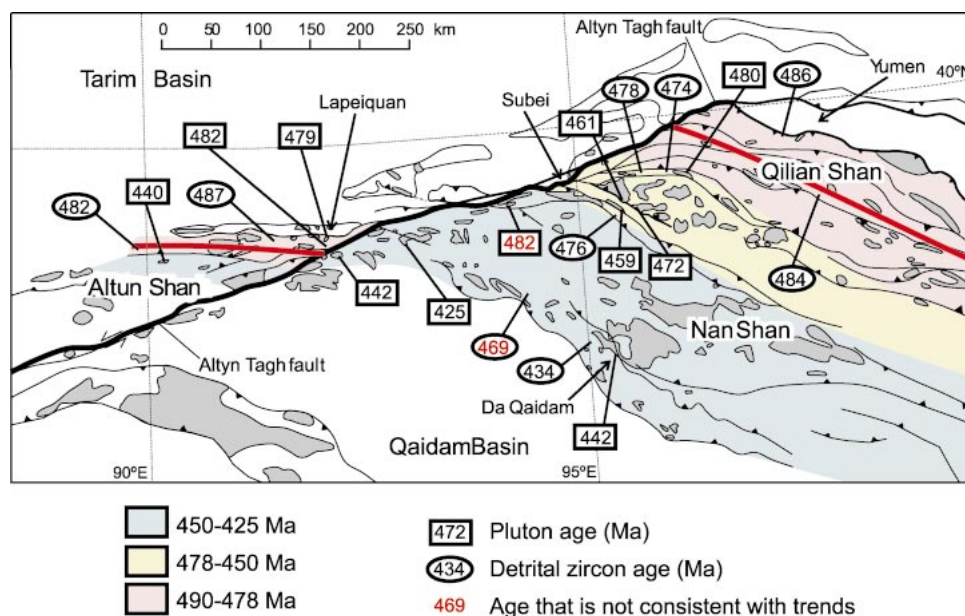


Figure 16. Map showing the ages of early Paleozoic detrital zircons (expressed in terms of “peak” ages from Fig. 11) and plutons (from Gehrels et al. [2003] and Cowgill et al. [2003]) in the study area. Two samples that do not fit within the three general age zones are highlighted in red. The age pattern south of the fault suggests that magmatism migrated southwestward during Ordovician–early Silurian time. The distance between 490–478 Ma magmatism north and south of the fault suggests that ~370 km of offset has occurred on the eastern segment of the Altn Tagh fault.

clude South China, North China, Australia, and related continental fragments.

3. Our detrital-zircon data are not consistent with previous models for early Paleozoic time in which the region either consisted of several distinct magmatic arcs separated by small ocean basins (archipelago model of Hsü et al., 1995) or grew southwestward from the Tarim and Sino-Korean cratons as a broad accretionary complex (Şengör and Natal'in, 1996). Following Sobel and Arnaud (1999), we suggest instead that the Qaidam and Qilian terranes formed a coherent crustal fragment separated from the Tarim and Sino-Korean cratons by an ocean basin of unknown size. This ocean basin is interpreted to have closed by southwest-dipping subduction beneath the Qaidam and Qilian terranes, producing the widespread Early Ordovician through Early Silurian magmatism, and then to have collided with the southwest margin of the Tarim and Sino-Korean cratons during middle Silurian through Early Devonian time (Fig. 17).

4. Our data also provide two new estimates for the offset along the eastern segment of the Altn Tagh fault. Correlation across the fault of shallow-marine quartzites that contain abundant ca. 1.9–1.1 Ga detrital zircons yields an offset of ~400 km, whereas alignment of regions that were sites of 490–478 Ma magmatism requires restoration of ~370 km of displacement. These offsets are very similar

to 350–400 km estimates reported by Molnar and Tapponnier (1975), Ritts and Biffi (2000, 2001), Sobel et al. (2001), Yang et al. (2001), and Yue et al. (2001).

APPENDIX 1. U-Pb GEOCHRONOLOGIC METHODS

For each sample, ~5 kg of material was collected from a single outcrop. The samples were processed in the field by using a portable rock grinder to break the rocks into sand-size material, disposable sieve screens to remove rock fragments, and a gold pan to concentrate the heavy minerals. Final mineral separation was accomplished with heavy liquids and a magnetic separator. Most zircon grains analyzed by ID-TIMS were abraded with an air-abrasion device (Krogh, 1982) prior to analysis.

The detrital-zircon populations were sieved into size fractions, and, unless otherwise noted, the analyzed grains were selected at random from the larger grain sizes available (generally >80 µm). The selection of only large grains may have biased the results of the study by increasing the representation of (1) coarse plutonic sources over fine-grained plutonic rocks or volcanic rocks, (2) nearby sources over distant sources, and (3) felsic igneous rocks over intermediate or mafic compositions. This selection criterion is necessary, however, because small grains are very difficult to analyze as single crystals and commonly yielded highly discordant ages.

Sixteen samples were analyzed by ID-TIMS, utilizing analytical methods described by Gehrels (2000). One additional sample was analyzed by laser-ablation multicollector inductively coupled plasma-mass spectrometry (LA-MC-ICP-MS). These analyses involve ablation of the zircon with

a New Wave DUV193 Excimer laser (operating at a wavelength of 193 nm) using a spot diameter of 50 µm. The analysis lasts for 20 s, during which a pit ~20 µm in depth is excavated. This ablated material is carried in argon gas into a Micromass IsoProbe, which is equipped with a flight tube of sufficient width that U and Pb isotopes are measured simultaneously. The measurements are made in static mode, by using Faraday detectors for ^{238}U , ^{232}Th , and ^{208}Pb – ^{206}Pb and an ion-counting channel for ^{204}Pb . Ion yields are ~1 mV per ppm. Common Pb corrections are made by using the measured ^{204}Pb and assuming initial Pb composition from Stacey and Kramers (1975). Interelement fractionation of U and Pb ranges up to 20%, whereas isotopic fractionation of Pb is generally <5%. In-run analysis of zircon grains of known isotopic and U-Pb composition (every fifth measurement) is used to correct for this fractionation. The resulting uncertainties are generally 2%–4% (2σ) for $^{207}\text{Pb}^*/^{206}\text{Pb}^*$ and $^{206}\text{Pb}^*/^{238}\text{U}$ ages (asterisks indicate that Pb has been corrected for common Pb) (Table DR2; see footnote 1).

The analytical data are presented in Table DR1 (for ID-TIMS analyses; see footnote 1) and Table DR2 (for ICP-MS analyses; see footnote 1). Unless otherwise noted, the ages used for provenance interpretation are $^{206}\text{Pb}^*/^{238}\text{U}$ ages for grains younger than 800 Ma and $^{207}\text{Pb}^*/^{206}\text{Pb}^*$ ages for grains older than 800 Ma. Concordia diagrams and relative-age-probability diagrams are presented for each sample (through the use of data-reduction and plotting programs of Ludwig, 1991a, 1991b, 2001). The relative-age-probability diagrams show each age and its uncertainty as a normal distribution and sum all ages in a sample (or set of samples) into a single curve. The curves are then divided by the number of constituent grains, such that each curve on a diagram contains the same area.

SW

NE

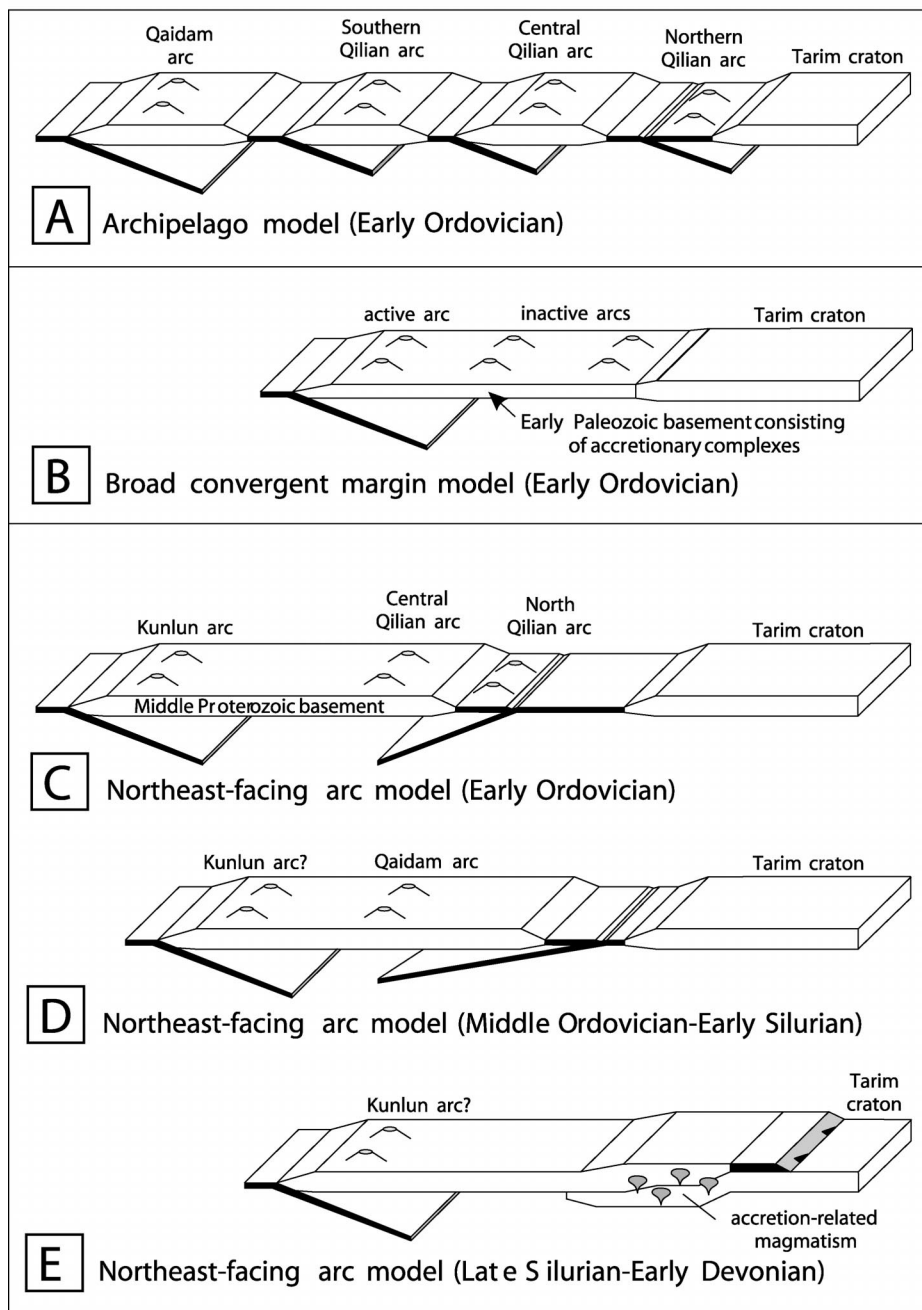


Figure 17. Tectonic models for the early Paleozoic tectonic evolution of rocks in the north-eastern Tibetan plateau. Directions shown are for present day. (A) Archipelago model, adapted from Hsü et al. (1995) and others. (B) Broad accretionary-complex model, adapted from Šenĝo and Natal'in (1996). (C–E) Preferred model, adapted from Sobel and Arnaud (1999), in which the Qaidam and Qilian terranes consist of a northeast-facing magmatic arc built on a basement of Middle Proterozoic age. Closure of the ocean basin along the leading edge of the Qilian-Qaidam terrane led to accretion against the southern margin of the Tarim and Sino-Korean cratons during Silurian–Devonian time.

APPENDIX 2. SAMPLE PETROGRAPHY, LOCATION INFORMATION, AND DETRITAL-ZIRCON CHARACTERISTICS

Our age samples were point-counted by using the Gazzi-Dickinson method (Ingersoll et al., 1984); we counted >400 points per sample. Framework grain types and graphical representations of the detrital modes and provenance fields are from Dickinson et al. (1983). The grain abundances, summed to 100%, are shown in Table A1. Following are the petrographic descriptions for each age sample.

Sample 1 (GA220, 39°17.256'N, 93°00.140'E)

This sample was collected from the easternmost Altun Shan, near the village of Annanba. The rock analyzed is a medium-grained quartz arenite that consists largely of well-rounded and highly spherical monocrystalline quartz grains. The only other framework grains recognized consist of lithic fragments of quartz-rich siltstone, although a high proportion of quartzose overgrowths may have obscured other original components. This sandstone occurs in beds that are 20–80 cm in thickness and locally contain pebbly horizons. Many sandstone beds contain cross-beds, and ripple marks are seen on bedding surfaces of finer-grained layers. It is presumed that this sequence accumulated in a shallow-marine setting either within or along the southern (in present coordinates) margin of the Tarim craton. Zircon grains in the sample are all well rounded and range from colorless to various shades of pink. A subordinate fraction consists of yellowish grains that are cloudy, presumably because of radiation damage.

Sample 2 (AY 6–6-02–2, 39°17.219'N, 92°41.542'E)

This is a medium-grained quartz arenite consisting mainly of subrounded monocrystalline quartz grains and small proportions of feldspar and quartzose siltstone fragments. Quartzose overgrowths are widespread. Zircons are all very well rounded, medium to dark pink grains.

Sample 3 (GA33, 38°47.067'N, 91°01.383'E)

This sample was collected from the western end of the Hati Shan. The rock is a fine-grained quartzite consisting predominantly of monocrystalline quartz grains and a subordinate fraction of plagioclase and muscovite-biotite schist fragments. Metamorphic muscovite makes up ~2% of the rock. Zircons in the sample are mainly colorless to light pink, but a small proportion of darker pink grains is also present. All of the grains are well rounded.

Sample 4 (GA209, 39°36.999'N, 96°12.075'E)

This sample consists of a predominant proportion of well-rounded and highly spherical monocrystalline quartz grains and of subordinate proportions of quartz arenaceous siltstone, muscovite-biotite schist, and felsic metavolcanic(?) fragments. Grain size is fine to medium. A matrix of microcrystalline calcite and sericite makes up a significant proportion of the rock. The sample was collected from the north side of the northern Daxue Shan. The sample yielded only small (<125 μm) zircon grains that range from well rounded to euhedral in morphology and from colorless to light pink in color.

TABLE A1. DETRITAL MODES OF SANDSTONES

Sample number	Qm	Qp	Kspar	Plag	Volc	Carb	Chert	Schist	Mica	Horn	Opaque	Matrix	Secondary minerals
1	62	5										25	7
2	83	<1	<1	2								14	
3	95			1				1				2	
4	70	6			1				1		1	19	1
5	74		16	5					2		1	2	
6	69		1	7	3							20	
7	12	6	7	12	41				<1			8	14
8	11	8		15	38				1		1	18	8
9	23	<1	7	31	18	<1			5		3	11	<1
10	20	<1	9	6	45	1				<1	4	14	
11	11	2		27	40					2	1	11	6
12	9	1	4	43	25						3	16	
13	25	9	<1	8	12	6	21	2				15	2
14	58	2	1	15	18				<1		<1	5	
15	56	3	2	8	17						1	6	6
16	42	5	4	1	24	5	1	<1			1	13	2

Notes: Grain populations summed to 100%. Grains include monocrySTALLINE quartz grains (Qm); polycrystalline quartzose lithic fragments (mainly siltstone) (Qp); K-feldspar (Kspar); plagioclase (Plag); lithic fragments of volcanic rocks (Volc), carbonate rocks (Carb), chert (probably includes siliceous argillite), schist, mica, and hornblende (Horn); and opaque minerals (Opaque). Matrix consists of quartz, feldspar, mica, carbonate, and/or chlorite, whereas secondary minerals consist of metamorphic muscovite and biotite in some samples and calcite in others. Note that the detrital modes have significant uncertainty in samples that have high percentages of matrix and/or secondary minerals.

Sample 5 (GA206, 38°49.095'N, 97°56.647'E)

This medium-grained quartz arenite consists predominantly of subrounded monocrySTALLINE quartz grains; subordinate fractions of K-feldspar, plagioclase, and detrital muscovite are also present. The sample was collected from the southwest flank of the Tulai Nan Shan. Zircons in the sample are all well rounded, and most are light pink in color.

Sample 6 (GA221, 39°13.421', 94°17.670')

This sample was collected from a thick sequence of metaturbidites that underlies the Danjin Shan and the northwestern Dang He Nan Shan. The strata are interpreted to be metaturbidites because most beds show strong size grading, from protoliths of coarse (locally pebbly) sand at the base to mudstone or shale at the top. Beds are commonly 20–50 cm in thickness. This uniform bedding and the variable resistance to erosion within individual beds creates a very distinctive outcrop pattern. The sample consists of fine-grained schistose quartzite that is metamorphosed to biotite-muscovite-quartz-plagioclase schist. Framework components include monocrySTALLINE quartz, plagioclase, and schistose mafic grains interpreted to have been derived from meta-volcanic fragments, but a significant percentage of the rock consists of metamorphic muscovite and quartz. Because of the degree of metamorphism, the modal components and proportions in this sample are highly uncertain. Zircons in the sample are uniformly light pink in color and moderately to well rounded.

Sample 7 (GA119, 39°02.788'N, 95°33.586'E)

This is a feldspar- and volcanic lithic-rich sandstone of coarse grain size. The sandstone occurs in beds 30–50 cm in thickness, many of which grade from coarse sand at the base to mudstone at the top. Some horizons contain pebbly bases and/or several-centimeter-scale angular rip-up clasts of intraformational clastic strata. The sequence also contains horizons of laminated gray mudstone. Prominent framework grains include feldspar-phenocryst-bearing

porphyritic felsic volcanic fragments and hornblende-bearing mafic volcanic fragments, as well as plagioclase, K-feldspar, and monocrySTALLINE quartz grains. A significant percentage of the rocks is made up of a microcrystalline matrix of quartz, feldspar, calcite, muscovite, and chlorite. The sample was collected from the east flank of the central Dang He Nan Shan. Zircons from the sample are generally light pink in color, and most grains are euhedral in morphology.

Sample 8 (GA132, 39°28.598'N, 95°48.934'E)

This is a coarse-grained sandstone that consists largely of volcanic lithic grains (derived from both felsic and mafic volcanic rocks), plagioclase, distinctively bluish microcrystalline quartz grains, and fragments of quartz arenaceous siltstone. There is also a significant proportion of matrix. The sandstone occurs in a sequence of graded beds that underlie much of the south flank of the eastern Yema Shan. Neither the base nor the top of the sequence was observed. Zircons in the sample are either euhedral and colorless to light pink or well rounded and pinkish.

Sample 9 (GA190, 39°03.632'N, 90°11.548'E)

This medium-grained sandstone consists of angular grains of plagioclase, K-feldspar, volcanic fragments (felsic compositions predominant over mafic compositions), and detrital muscovite, as well as subrounded monocrySTALLINE quartz grains. Sandstone in the lower part of the sequence is cross-bedded. Zircons in the sample are light pink in color and euhedral in shape.

Sample 10 (GA204, 39°00.871'N, 98°05.370'E)

This coarse-grained sandstone consists predominantly of felsic and mafic volcanic fragments and of lesser proportions of monocrySTALLINE quartz, plagioclase, and K-feldspar. Conglomeratic layers consist mainly of mafic volcanic clasts that locally reach 20 cm in diameter. Our sample was collected from exposures along the Tulai River. Zircons in

this sample are colorless and euhedral, and all grains were abraded prior to analysis.

Sample 11 (GA214, 39°00.871'N, 98°05.370'E)

This sandstone is coarse grained and consists largely of felsic volcanic fragments and plagioclase; subordinate mafic volcanic fragments and monocrySTALLINE quartz grains also occur. Our sample was collected from the west flank of the Serteng Shan. Zircons in the sample are mostly colorless and euhedral; a small proportion of light pink, well-rounded grains are also present. Surprisingly, in light of the coarse grain size of the sampled sandstone, all of the zircons extracted from this sample were <100 μm in length. Only the larger grains were abraded prior to analysis.

Sample 12 (GA201, 39°39.726'N, 97°35.592'E)

This medium-grained sandstone consists mainly of plagioclase grains (commonly as phenocrysts in volcanic fragments), volcanic fragments derived mainly from felsic source rocks, and subordinate K-feldspar and monocrySTALLINE quartz grains. Most of the sequence consists of siltstone-mudstone turbidites; sandstone occurs only rarely at the base of some beds. Zircons in this sample are all colorless and euhedral and were abraded prior to analysis.

Sample 13 (GA210, 39°31.466'N, 96°08.935'E)

This coarse-grained sandstone contains monocrySTALLINE quartz and plagioclase grains as well as abundant fragments of chert, quartz arenaceous siltstone, and volcanic rocks. Subordinate but important additional components include fragments of carbonate and argillite. Bedding in the sandstone ranges from 10 to 30 cm in thickness. Most beds show strong size grading, from coarse sandstone upward into siltstone and mudstone. Pebbly horizons occur near the base of the sequence. Layers of mafic volcanic flows and breccia occur in the sequence as well. The sample was collected from the south side of the northwestern Daxue Shan. Zircons in the sample are quite variable in color (ranging from colorless to light pink) and in morphology (ranging from euhedral to well rounded).

Sample 14 (GA174, 39°06.567'N, 91°27.830'E)

This fine-grained sandstone is highly recrystallized; secondary calcite and muscovite overprint much of the rock. Obvious framework components include monocrySTALLINE quartz and plagioclase grains. A significant proportion of the rock is made up of angular detrital fragments that consist mostly of secondary minerals, but locally display primary(?) quartzofeldspathic groundmass containing feldspar phenocrysts. These fragments are interpreted to have been derived from felsic volcanic fragments. Most beds in the sequence are graded from coarse sandstone to mudstone and average ~30 cm in thickness. Interlayered with the sandstones are interbeds of laminated mudstone. Our sample was collected from the south side of the Jinyan Shan, in the Altun Shan (Fig. 2), from a sequence that is at least 2 km in thickness. Zircons in the sample are mostly light pink and euhedral; subordinate populations are rounded, colorless, and/or darker pink in color.

Sample 15 (GA212, 38°02.501'N, 95°09.282'E)

This medium-grained quartzite is highly deformed and consists of a large proportion of secondary muscovite and calcite. Quartz, plagioclase, and K-feldspar are obvious detrital components, and volcanic fragments are interpreted to be present on the basis of the occurrence of angular detrital fragments that display feldspar or hornblende phenocrysts in a quartzofeldspathic or chloritic groundmass. These metasediments are interbedded with conglomeratic beds near the base of a clastic section that rests on felsic and mafic metavolcanic rocks. Clasts in the conglomerate consist of metarhyolite, metabasalt, and vein quartz that range up to 20 cm in diameter. The conglomeratic strata grade up section into siltstone and mudstone. Our sample was collected from a sandstone layer ~10 m above the basal contact. Zircons in this unit are mainly light pink in color and well rounded; a smaller proportion of the zircon population is colorless and/or euhedral. Our sample was collected from the western flank of the Qaidam Shan.

Sample 16 (GA200, 40°03.184'N, 97°23.021'E)

This pebbly sandstone consists mainly of monoclinic quartz grains, primarily felsic and less commonly mafic volcanic fragments, K-feldspar, and plagioclase. Minor but important additional components include fragments of quartz arenaceous siltstone, carbonate, chert, and muscovite schist. The horizon sampled is a coarse-grained immature sandstone containing detrital feldspar and mica. It is interlayered with thin conglomerate horizons that contain pebbles (up to 5 cm across) of plutonic rocks that range from granite to diorite in composition. Zircons in the sample are colorless and euhedral.

Sample 17 (GA182, 38°54.202'N, 91°32.318'E)

This sample comes from quartz-phenocryst-bearing porphyritic metarhyolite that contains both reddish and greenish horizons. The metarhyolite occurs as a sill within a thick sequence of biotite phyllite (derived from banded mudstone), stromatolitic marble, and rare quartzite layers. Zircons extracted from the metarhyolite are colorless to light pink in color and euhedral in morphology.

ACKNOWLEDGMENTS

This research was conducted as part of a collaborative project of the University of Arizona, the University of California at Los Angeles, Arizona State University, and the Institute of Geomechanics in Beijing. Funding was provided by the Continental Dynamics Program of the National Science Foundation (EAR-9725663). We thank Robert Butler, Guillaume Dupont-Nivet, and Chen Xunhua for their assistance in the field. Bill Dickinson assisted in petrographic aspects of the study. Alex Pullen provided very capable assistance with processing the U-Pb samples, and Jeff Vervoort's guidance in conducting the ICP-MS analyses was essential. We thank Paul Kapp, Steve Graham, and Nicholas Arnaud for very helpful reviews.

REFERENCES CITED

Cowgill, E., Yin, A., Harrison, T.M., and Wang, X.-F., 2003, Reconstruction of the Altyn Tagh fault based on U-Pb geochronology: The role of backthrusts, mantle sutures, and heterogeneous crustal strength in forming

the Tibetan plateau: *Journal of Geophysical Research* (in press).

Delville, N., Arnaud, N., Montel, J.-M., Roger, F., Brunel, M., Tapponnier, P., and Sobel, E., 2001, Paleozoic to Cenozoic deformation along the Altyn Tagh fault in the Altun Shan massif area, eastern Qilian Shan, northeast Tibet, China, in Hendrix, M.S., and Davis, G.A., eds., *Paleozoic and Mesozoic tectonic evolution of central Asia: From continental assembly to intracontinental deformation: Geological Society of America Memoir 194*, p. 269–292.

Dickinson, W.R., Beard, L.S., Brakenridge, G.R., Erjavec, J.L., Ferguson, R.C., Inman, K.F., Knapp, R.A., Lindberg, F.A., and Ryberg, P.T., 1983, Provenance of North American Phanerozoic sandstones in relation to tectonic setting: *Geological Society of America Bulletin*, v. 94, p. 222–235.

Gehrels, G.E., 2000, Introduction to detrital zircon studies of Paleozoic and Triassic strata in western Nevada and northern California, in Soreghan, M.J., and Gehrels, G.E., eds., *Paleozoic and Triassic paleogeography and tectonics of western Nevada and northern California: Geological Society of America Special Paper 347*, p. 1–17.

Gehrels, G.E., Yin, A., and Wang, X.-F., 2003, Magmatic history of the northeastern Tibetan plateau: *Journal of Geophysical Research* (in press).

Harris, N.B.W., Xu, R., Lewis, C.L., Hawke, C.J., and Zhang, Y., 1988, Isotope geochemistry of the 1985 Tibet Geotraverse, Lhasa to Golmud: *Royal Astronomical Society Geophysical Journal, Ser. A*, v. 327, p. 263–285.

Hsü, K.J., Guitang, P., and Şenğör A.M.C., 1995, Tectonic evolution of the Tibetan plateau: A working hypothesis based on the archipelago model of orogenesis: *International Geology Review*, v. 37, p. 473–508.

Ingersoll, R.V., Bullard, T.F., Ford, R.L., Grimm, J.P., Pickle, J.D., and Sares, S.W., 1984, The effect of grain size on detrital modes: A test of the Gazi-Dickinson point-counting method: *Journal of Sedimentary Petrology*, v. 54, p. 103–116.

Krogh, T.E., 1982, Improved accuracy of U-Pb zircon ages by the creation of more concordant systems using an air abrasion technique: *Geochimica et Cosmochimica Acta*, v. 46, p. 637–649.

Li, C.Y., Liu, Y., Zhu, B.C., Feng, Y.M., and Wu, H.C., 1978, Structural evolution of Qilian and Qilian Shan, in *Scientific papers in geology and international exchange: Beijing*, Geologic Publishing House, p. 174–197.

Liu, Z.Q., 1988, Geologic map of the Qinghai-Xizang (Tibetan) plateau and adjacent areas: Beijing, Geological Publishing House, Chengdu Institute of Geology and Mineral Resources, scale 1:1,500,000.

Ludwig, K.R., 1991a, A computer program for processing Pb-U-Th isotopic data: U.S. Geological Survey Open-File Report 88–542.

Ludwig, K.R., 1991b, A plotting and regression program for radiogenic-isotopic data: U.S. Geological Survey Open-File Report 91–445.

Ludwig, K.R., 2001, *Isoplot/Ex*, rev. 2.49: Berkeley Geochronology Center, Special Publication 1A, 56 p.

Métivier, F., Gaudemer, Y., Tapponnier, P., and Meyer, B., 1998, Northeastward growth of the Tibet plateau deduced from balanced reconstructions of two depositional areas: The Qaidam and Hexi Corridor basins, China: *Tectonics*, v. 17, p. 823–842.

Meyer, B., Tapponnier, P., Gaudemer, Y., Peltzer, G., Guo, S., and Chen, Z., 1996, Rate of left-lateral movement along the easternmost segment of the Altyn Tagh fault, east of 96°E (China): *Geophysical Journal International*, v. 124, p. 29–44.

Meyer, B., Tapponnier, P., Bourjot, L., Métivier, F., Gaudemer, Y., Peltzer, G., Guo, S., and Chen, Z., 1998, Crustal thickening in Gansu-Qinghai, lithospheric mantle subduction, and oblique, strike-slip controlled growth of the Tibet plateau: *Geophysical Journal International*, v. 135, p. 1–47.

Molnar, P., and Tapponnier, P., 1975, Cenozoic tectonics of Asia: Effects of a continental collision: *Science*, v. 189, p. 419–426.

Peltzer, G., and Tapponnier, P., 1988, Formation and evolution of strike-slip faults, rifts, and basins during In-

dia-Asia collision: An experimental approach: *Journal of Geophysical Research*, v. 93, p. 15,085–15,117.

Ritts, B.D., and Biffi, U., 2000, Magnitude of post-Middle Jurassic (Bajocian) displacement on the Altyn Tagh fault, northwest China: *Geological Society of America Bulletin*, v. 112, p. 61–74.

Ritts, B.D., and Biffi, U., 2001, Mesozoic northeast Qaidam basin: Response to contractional reactivation of the Qilian Shan, and implications for the extent of Mesozoic intracontinental deformation in central Asia, in Hendrix, M.S., and Davis, G.A., eds., *Paleozoic and Mesozoic tectonic evolution of central Asia: From continental assembly to intracontinental deformation: Geological Society of America Memoir 194*, p. 293–316.

Scotese, C.R., 2002, Earth history reconstructions: <http://www.scotese.com/earth.htm>.

Şenğör A.M.C., and Natal'in, B.A., 1996, Paleotectonics of Asia: Fragments of a synthesis, in Yin, A., and Harrison, T.M., eds., *The tectonics of Asia: New York*, Cambridge University Press, p. 486–640.

Sobel, E.R., and Arnaud, N., 1999, A possible middle Paleozoic suture in the Altyn Tagh, northwest China: *Tectonics*, v. 18, p. 64–74.

Sobel, E.R., Arnaud, N., Jolivet, M., Ritts, B.D., and Brunel, M., 2001, Jurassic to Cenozoic exhumation history of the Altyn Tagh range, northwest China, constrained by ⁴⁰Ar/³⁹Ar and apatite fission track thermochronology, in Hendrix, M.S., and Davis, G.A., eds., *Paleozoic and Mesozoic tectonic evolution of central Asia: From continental assembly to intracontinental deformation: Geological Society of America Memoir 194*, p. 247–267.

Stacey, J.S., and Kramers, J.D., 1975, Approximation of terrestrial lead isotope evolution by a two-stage model: *Earth and Planetary Science Letters*, v. 26, p. 207–221.

Tapponnier, P., Meyer, B., Avouac, J.P., Peltzer, G., Gaudemer, Y., Shunmin, G., Hongfa, X., Kelun, Y., Zhitai, C., Shuhua, C., and Huagang, D., 1990, Active thrusting and folding in the Qilian Shan, and decoupling between upper crust and mantle in northeastern Tibet: *Earth and Planetary Science Letters*, v. 97, p. 382–403.

Tapponnier, P., Zhiqin, X., Roger, F., Meyer, B., Arnaud, N., Wittlinger, G., and Jingsui, Y., 2001, Oblique stepwise rise and growth of the Tibet plateau: *Science*, v. 294, p. 1671–1677.

Tucker, R.D., and McKerrow, W.S., 1995, Early Paleozoic chronology: A review in light of new U-Pb zircon ages from Newfoundland and Britain: *Canadian Journal of Earth Sciences*, v. 32, p. 368–379.

Xia, L., Xia, Z., and Xu, X., 1996, Origin of the oceanic island arc system in the northern Qilian Shan: Beijing, Geological Publishing House, 153 p.

Xiong, J., and Coney, P.J., 1985, Accreted terranes of China, in Howell, D.G., ed., *Tectonostratigraphic terranes of the Circum-Pacific region: Houston, Circum-Pacific Council for Energy and Mineral Resources, Earth Science Series*, no. 1, p. 349–361.

Xu, Z., Zhang, J., and Li, H., 2000, Architecture and orogeny of the northern Qilian orogenic belt, northwestern China: *Geological Society of China Journal*, v. 43, p. 125–141.

Yang, J., Xu, Z., Zhang, J., Chu, C.-Y., Zhang, R., and Liou, J.G., 2001, Tectonic significance of early Paleozoic high-pressure rocks in Altun-Qaidam-Qilian Mountains, northwest China, in Hendrix, M.S., and Davis, G.A., eds., *Paleozoic and Mesozoic tectonic evolution of central Asia: From continental assembly to intracontinental deformation: Geological Society of America Memoir 194*, p. 151–170.

Yin, A., and Harrison, T.M., 2000, Geologic evolution of the Himalayan-Tibetan orogen: *Annual Review of Earth and Planetary Sciences*, v. 28, p. 211–280.

Yue, Y., Ritts, B.D., and Graham, S.A., 2001, Initiation and long-term slip history of the Altyn Tagh fault: *International Geology Review*, v. 43, p. 1–7.

MANUSCRIPT RECEIVED BY THE SOCIETY 15 MARCH 2002
REVISED MANUSCRIPT RECEIVED 22 DECEMBER 2002
MANUSCRIPT ACCEPTED 19 JANUARY 2003

Printed in the USA